AMERICAN SOCIETY FOR MICROBIOLOGY | Applied and Environmental Microbiology®

BIODEGRADATION

Diesel and Crude Oil Biodegradation by Cold-Adapted Microbial Communities in the Labrador Sea

Sean M. C. Murphy,[a] María A. Bautista,[a] Margaret A. Cramm,[a]* Casey R. J. Hubert[a]

[a]Department of Biological Sciences, University of Calgary, Calgary, Alberta, Canada

ABSTRACT Oil spills in the subarctic marine environment off the coast of Labrador, Canada, are increasingly likely due to potential oil production and increases in ship traffic in the region. To understand the microbiome response and how nutrient biostimulation promotes biodegradation of oil spills in this cold marine setting, marine sediment microcosms amended with diesel or crude oil were incubated at *in situ* temperature (4°C) for several weeks. Sequencing of 16S rRNA genes following these spill simulations revealed decreased microbial diversity and enrichment of putative hydrocarbonoclastic bacteria that differed depending on the petroleum product. Metagenomic sequencing revealed that the genus *Paraperlucidibaca* harbors previously unrecognized capabilities for alkane biodegradation, which were also observed in *Cycloclasticus*. Genomic and amplicon sequencing together suggest that *Oleispira* and *Thalassolituus* degraded alkanes from diesel, while *Zhongshania* and the novel PGZG01 lineage contributed to crude oil alkane biodegradation. Greater losses in PAHs from crude oil than from diesel were consistent with *Marinobacter*, *Pseudomonas*_D, and *Amphritea* genomes exhibiting aromatic hydrocarbon biodegradation potential. Biostimulation with nitrogen and phosphorus (4.67 mM NH_4Cl and 1.47 mM KH_2PO_4) was effective at enhancing *n*-alkane and PAH degradation following low-concentration (0.1% [vol/vol]) diesel and crude oil amendments, while at higher concentrations (1% [vol/vol]) only *n*-alkanes in diesel were consumed, suggesting toxicity induced by compounds in unrefined crude oil. Biostimulation allowed for a more rapid shift in the microbial community in response to petroleum amendments, more than doubling the rates of CO_2 increase during the first few weeks of incubation.

IMPORTANCE Increases in transportation of diesel and crude oil in the Labrador Sea will pose a significant threat to remote benthic and shoreline environments, where coastal communities and wildlife are particularly vulnerable to oil spill contaminants. Whereas marine microbiology has not been incorporated into environmental assessments in the Labrador Sea, there is a growing demand for microbial biodiversity evaluations given the pronounced impact of climate change in this region. Benthic microbial communities are important to consider given that a fraction of spilled oil typically sinks such that its biodegradation occurs at the seafloor, where novel taxa with previously unrecognized potential to degrade hydrocarbons were discovered in this work. Understanding how cold-adapted microbiomes catalyze hydrocarbon degradation at low *in situ* temperature is crucial in the Labrador Sea, which remains relatively cold throughout the year.

KEYWORDS Labrador Sea, subarctic, bioremediation, biostimulation, hydrocarbonoclastic bacteria, metagenomics, oil spill

The Labrador Sea (Fig. 1) faces heightened oil spill risk as shipping traffic in the region increases in response to longer ice-free seasons within connected Arctic corridors (1–3). In addition, oil production offshore Labrador is expected to increase with the government of Newfoundland and Labrador planning to double its extraction of

Citation Murphy SMC, Bautista MA, Cramm MA, Hubert CRJ. 2021. Diesel and crude oil biodegradation by cold-adapted microbial communities in the Labrador Sea. Appl Environ Microbiol 87:e00800-21. https://doi.org/10.1128/AEM.00800-21.

Editor Jeremy D. Semrau, University of Michigan—Ann Arbor

Copyright © 2021 Murphy et al. This is an open-access article distributed under the terms of the Creative Commons Attribution 4.0 International license.

Address correspondence to Sean M. C. Murphy, sean.murphy1@ucalgary.ca, or Casey R. J. Hubert, chubert@ucalgary.ca.

* Present address: Margaret A. Cramm, Queen Mary University of London, London, United Kingdom.

Received 27 April 2021
Accepted 24 July 2021
Accepted manuscript posted online 11 August 2021
Published 28 September 2021

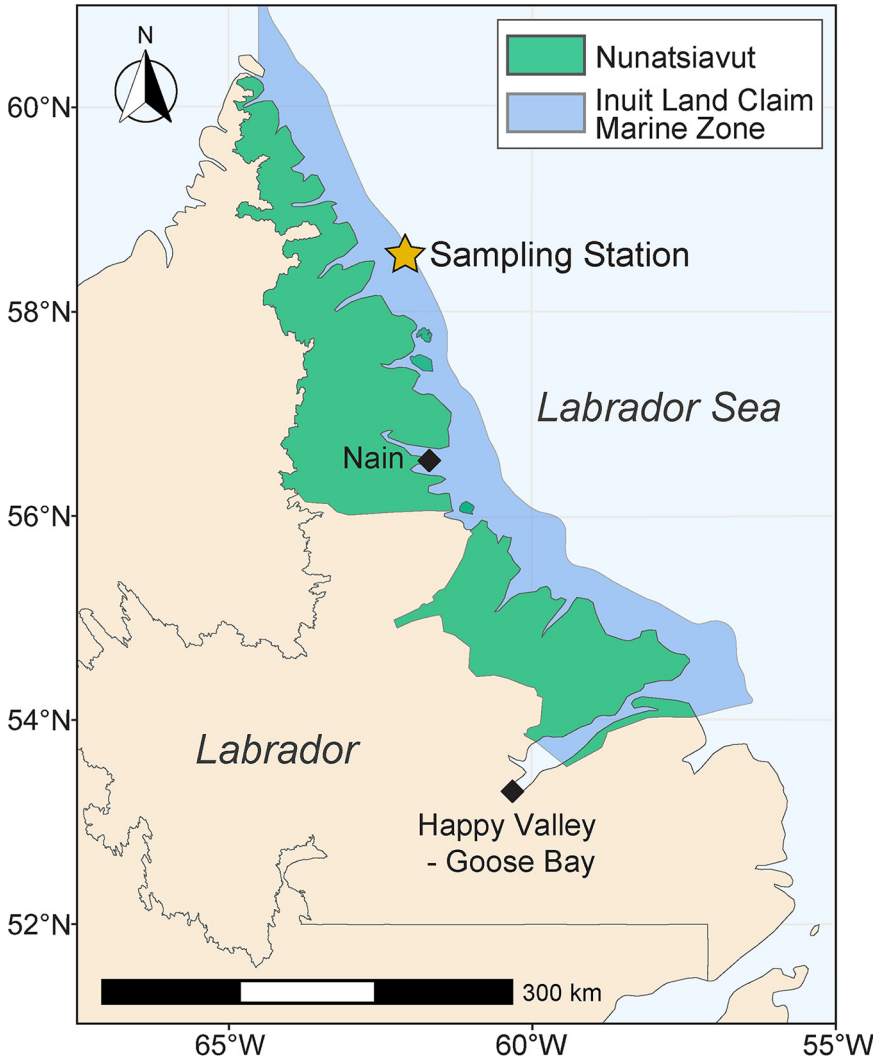

FIG 1 Map of Labrador and the Labrador Sea. Sampling station (star) marks where marine sediment was collected in triplicate in 2015 (cross-reference with Table S1 in the supplemental material). Sampling occurred within the marine zone of the Nunatsiavut Inuit Land Claim Agreement (blue shaded area along the coast).

the resource by the year 2030. Oil spill research has expanded rapidly over the past decade, better equipping jurisdictions to manage future spills (4). The behavior and fate of spilled oil in the Labrador Sea, however, remains difficult to predict on account of accessibility to the area, cold ocean temperature, and prolific sea ice. A better understanding of oil spill dynamics in this region and other subarctic areas should help in managing future oil releases in these vulnerable environments.

Oil contamination leaves a lasting impact on northern ecosystems already facing cumulative negative effects from climate change, pollution, and overexploitation of resources (5, 6). Despite the heavy occurrence of icebergs, first year sea ice, and an increasing occurrence of mobile Arctic multiyear sea ice (7) in the Labrador Sea, current environmental assessment reports for the region highlight a "limited knowledge base" regarding oil spills in ice impacted waters (8). Concerns have been expressed by Labradoreans over the impact that an oil spill may have on coastal areas (8) given bioaccumulation of petroleum constituents within fish and other marine wildlife that local communities rely on for food (5). Labrador's remoteness and distance from oil spill response resources located in more southern cities and ports (i.e., St. John's) make local wildlife and coastal communities inhabited by Nunatsiavut Inuit, the Southern Inuit of NunatuKavut, and

Sheshatshiu and Mushuau Innu, more vulnerable to oil spill contaminants. The 1989 Exxon Valdez oil spill underscored the significant risks to shoreline ecosystems posed by transporting crude oil via ocean shipping (9). In addition, the Canadian Coast Guard has voiced concern over spills of diesel because of its heavy use as the fuel for maritime transportation in the Arctic, because of its eventual replacement of bunker fuel in larger cargo ships, and because of the high volumes of diesel shipped by sea for electricity generation in northern communities (10).

With increasing oil spill risk there is a growing need for reliable marine bioindicators of environmental impact (11, 12) and effective strategies for dealing with hydrocarbon contaminants in the environment (13–16). Microbial responses to hydrocarbons have been studied thoroughly (17) with over 330 genera of *Bacteria* and *Archaea* identified with metabolisms, degradation pathways, and genes involved in hydrocarbon oxidation (18). Hydrocarbonoclastic bacteria (HCB), a large proportion of which are members of the class *Gammaproteobacteria*, can use multiple carbon sources but display a preference for hydrocarbons (19). Some HCB, mostly marine bacteria, have been described as obligate, i.e., they use hydrocarbons almost exclusively (20). *Alcanivorax* and *Cycloclasticus* are commonly detected in oil spill studies and are typically implicated in the biodegradation of alkane and cyclic hydrocarbons, respectively (21). Other groups often considered obligate, such as *Oleiphilus*, *Oleispira*, and *Thalassolituus*, are also commonly enriched in the marine environment following oil spills (19–21). Despite being present in low abundance initially, accidental releases of oil provoke rapid proliferation of these and other hydrocarbon-degrading taxa (22, 23).

Low temperatures affect rates of oil biodegradation by reducing the solubility of certain oil compounds (24). This is especially important given that sea surface temperatures along the Labrador Shelf remain relatively cold throughout the year, ranging from –2°C to 10°C (8). Microbial communities capable of responding to hydrocarbons at low temperature can differ from those that respond at higher temperatures (25–27). HCB responses also depend on the concentration of hydrocarbons released to the environment (28) and the composition of the petroleum product, i.e., its proportion of alkanes (29) and aromatic hydrocarbons (24, 30). The rate and extent of oil degradation can also be limited by the low abundance of nitrogen (N) and phosphorus (P) in marine environments (31, 32). While spilled oil provides a rich carbon and energy source for HCB, it contains minimal available N and P for meeting the requirements that all microorganisms share for synthesizing nucleic acids and proteins. For every gram of hydrocarbon consumed, microorganisms require ~150 mg N and ~30 mg P (33, 34). Adding N and P following an oil spill allows indigenous microbial populations to overcome these environmental limitations. This biostimulation strategy was successfully employed in response to the Exxon Valdez oil spill, using the fertilizer Inipol EAP 22 (35).

In an open ocean context, sinking oil constitutes a considerable fraction of major spills, i.e., 25% during Ixtoc I (36) and an estimated 15% during Deepwater Horizon (11, 37). Partitioning of hydrocarbons between sediments and adjacent food webs represents an important exposure route (38) leading to disease, impaired health, and mortality in a wide range of organisms (39). Hydrocarbon biodegradation by benthic microbial communities is an important consideration when assessing the fate of oil in areas where shipping traffic and oil production are expected to increase. This is the first study to uncover how cold-adapted microbial communities in the Labrador Sea respond to hydrocarbon inputs of diesel or crude oil, as well as nutrient stimulation.

RESULTS

Biostimulation for diesel fuel and crude oil biodegradation. Nutrient addition enhanced low temperature (4°C) biodegradation of *n*-alkanes (C_{12}-C_{25}) in all diesel- or crude oil-amended microcosms but had the least impact on 1% crude oil, as revealed by gas chromatography-mass spectrometry (GC-MS) (Fig. 2A to D). This effect is evident in the ratio of *n*-C_{17}/pristane decreasing in all diesel amendments, but only in the 0.1% crude oil amendments (see Table S2). Alkanes were significantly more degraded

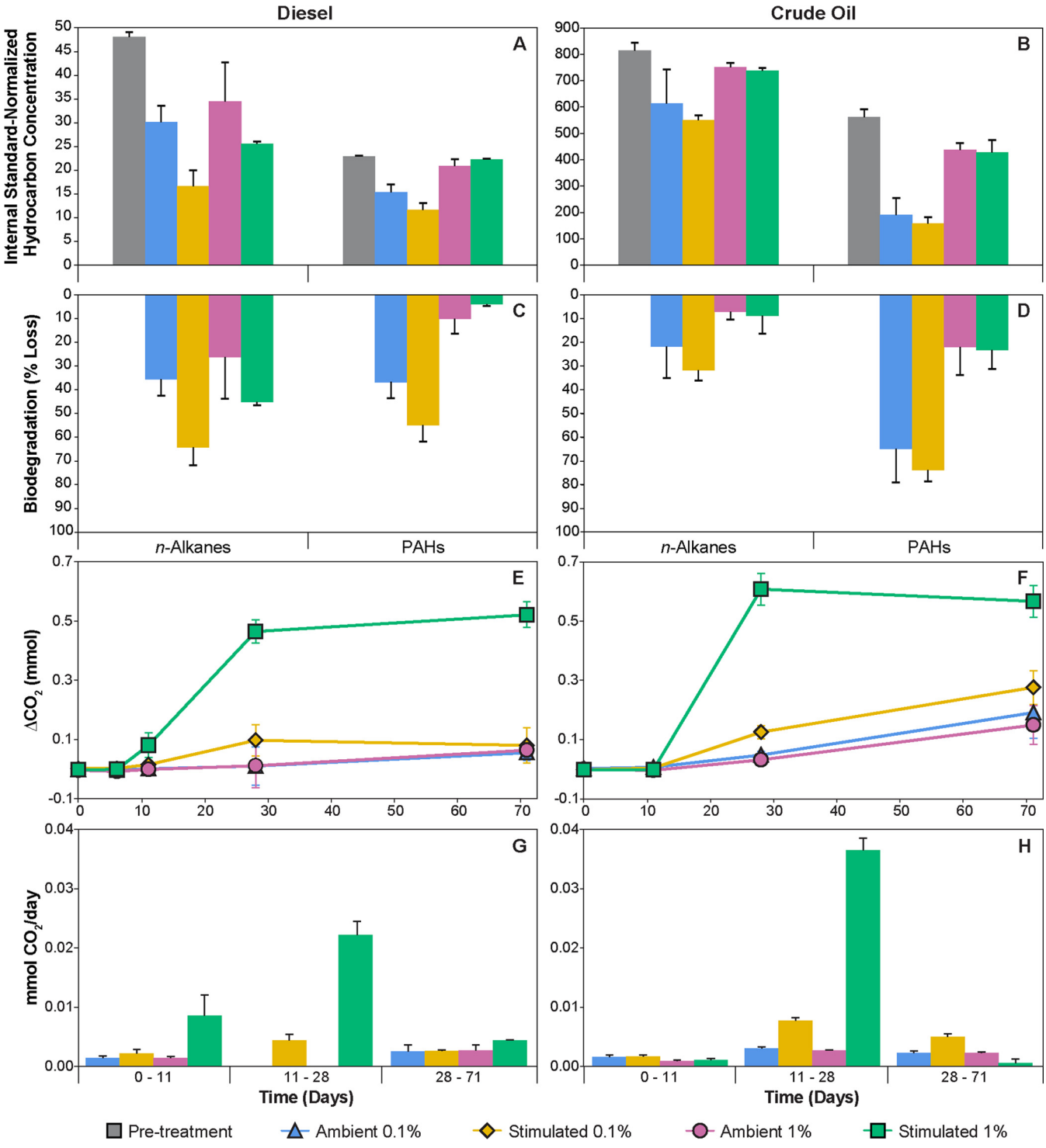

FIG 2 Hydrocarbon biodegradation within 0.1 and 1% (vol/vol) diesel (A, C, E, and G)- and crude oil (B, D, F, and H)-amended microcosms with nutrient stimulation or without (ambient). (A and B) Concentration of hydrocarbon compound groups at day 0 (pre-treatment) and after 71 days of incubation at 4°C. Hydrocarbon concentrations in diesel were obtained by normalizing compound peak areas against 1,3+3,9+2,10+3,10-dimethylphenanthrene, and in crude oil by normalizing against 17α(H),21β(H)-hopane. (C and D) Biodegradation conveyed as losses of measured *n*-alkanes (C_{12}-C_{25}) and PAHs from pre-treatment levels. (E to H) CO_2 production (E and F) determined by GC is plotted as the difference between hydrocarbon-amended and -unamended microcosms and was used to estimate rates of CO_2 production associated with hydrocarbon biodegradation (G and H) (CO_2 concentrations for unamended controls are shown in Fig. S1). Error bars represent standard errors of triplicate microcosms of the same treatment.

in diesel (43% loss) than crude oil (17% loss) ($F_{1,21}$ = 11.97, P = 0.002), despite comprising a similar initial proportion of the total measured hydrocarbons in both cases (Fig. 2A and B). Biostimulation also promoted biodegradation of polycyclic aromatic hydrocarbons (PAHs) in the presence of low (0.1%) but not high (1%) concentrations of diesel or crude oil (Fig. 2A to D), as reflected by 2MN/1MN ratios (see Table S2 in the supplemental material). PAHs were significantly more biodegraded in 0.1% crude oil (70%) than 0.1% diesel (46%) ($F_{1,9}$ = 8.96, P = 0.02).

Effects of hydrocarbon biodegradation stimulated by nutrient addition were also monitored by assessing headspace O_2 consumption and CO_2 production (Fig. 2E and F; see also Fig. S1 in the supplemental material). Biostimulation resulted in significantly more CO_2 generation among 1% diesel and crude oil amendments incubated at 4°C. Nutrient stimulation further increased rates of CO_2 generation, which reached maximum levels between 11 and 28 days in both 0.1 and 1% amendments. No significant changes in CO_2 were observed in any sediment-free or killed control microcosms (see Fig. S1E, F, I, and J). The combination of nutrient stimulation with 1% diesel led to complete oxygen consumption after 28 days (see Fig. S1E), resulting in anoxic conditions impacting subsequent CO_2 generation in these microcosms. There was no difference in CO_2 production between 0.1 and 1% amendments in the presence of ambient levels of nutrients, suggesting that seawater concentrations of N and P are limiting and require replenishment in order for microbial communities to contend with larger petroleum inputs. Ammonium-N persisted in the ambient nutrient control microcosms that were not amended with diesel or crude oil and in all nutrient-stimulated treatments whether amended with petroleum or not (see Fig. S2).

Microbial community changes in response to hydrocarbon input and biostimulation. Microbial community structure during 71 days of 4°C incubation was heavily influenced by both the type and concentration of petroleum product and whether nutrients were added in the presence of hydrocarbons (Fig. 3A). Nonmetric multidimensional scaling (NMDS) of Bray-Curtis dissimilarity revealed unincubated (day 0) and all unamended communities (28 and 71 days, regardless of nutrient stimulation) cluster together, signifying little community change in the absence of hydrocarbons (Fig. 3A, "unamended" ellipse; R-stat = 0.3, P = 0.001). The introduction of diesel or crude oil significantly influenced community structure (r^2 = 0.57, P = 0.001), resulting in clusters according to diesel or crude oil amendment that were significantly dissimilar from each other (R-stat = 0.667, P = 0.001) and from the community structure in unamended microcosms (Fig. 3A; see also Data Set S3). Higher concentrations of diesel or crude oil were significantly correlated with changes in community structure (r^2 = 0.45, P = 0.001) with significant dissimilarity between communities in 0.1 and 1% amended microcosms, particularly within the crude oil cluster (R-stat = 0.52, P = 0.001) more than the diesel cluster (R-stat = 0.25 P = 0.001). Nutrient stimulation also influenced these communities (r^2 = 0.34, P = 0.001), which were significantly dissimilar between ambient and nutrient stimulated treatments within the diesel cluster (R-stat = 0.39, P = 0.001) more than the crude oil cluster (R-stat = 0.1468, P = 0.026).

Microbial α-diversity was greatest prior to incubation or amendment with petroleum products, as revealed by the Shannon Index (Fig. 3B) and the number of operational taxonomic units (OTUs) (see Fig. S3). No significant changes in either of these parameters were observed throughout 71 days of 4°C incubation in the unamended controls, whereas diversity always dropped in the presence of diesel or crude oil regardless of their concentrations or nutrient biostimulation. Microbial community structure (Fig. 3A) and α-diversity (Fig. 3B) exhibited the largest changes within the first 28 days of incubation, concomitant with the highest rates of CO_2 generation (Fig. 2E and F). Microbial communities in diesel-amended microcosms shifted more within the first 28 days of incubation (R-stat = 0.3, P = 0.001) and experienced the greatest declines in Shannon Index (Fig. 3B) and OTU richness (see Fig. S3), compared to the 28- to 71-day period (R-stat = 0.07, P = 0.09), suggesting little change in the microbial community during the later interval. While hydrocarbon-amended and nutrient-stimulated microcosms exhibited the greatest declines in diversity, nutrient stimulation also resulted in the highest

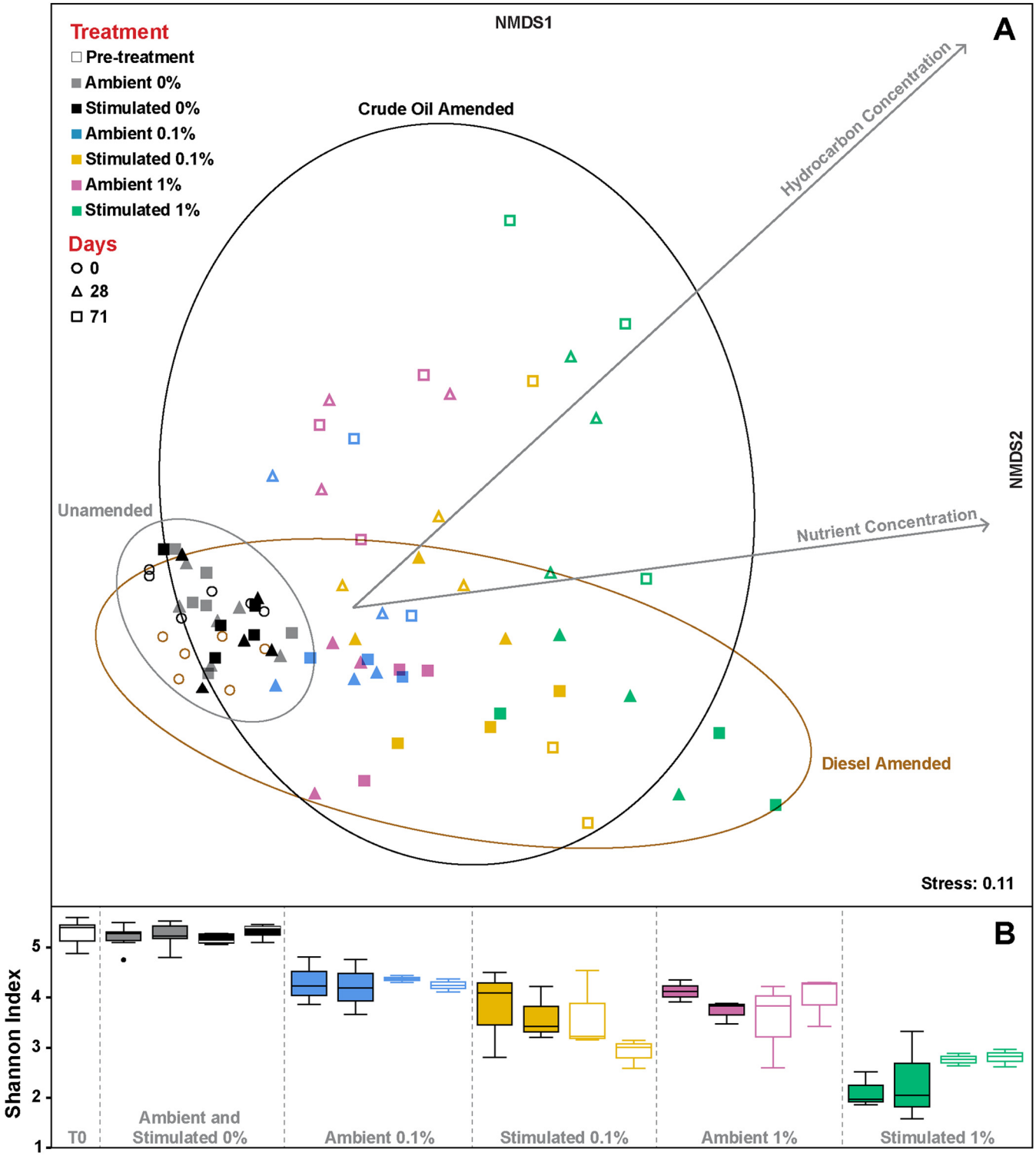

FIG 3 (A) Microbial community structure similarity among unamended (black and gray points), diesel-amended (solid-color points) and crude oil-amended (unfilled colored points) Labrador sediment microcosms incubated at 4°C for 71 days visualized by nonmetric multidimensional scaling (NMDS) of Bray-Curtis values for each community using 0.95 confidence cutoffs (ellipses). The lengths of the two factor arrows indicate the contribution of hydrocarbon and nutrient concentration variables to the dissimilarity between treatment group microbial communities. Significant fit and strong correlation were observed with hydrocarbon concentration (r^2 = 0.45, P = 0.001), nutrient concentration (r^2 = 0.34, P = 0.001), and type of petroleum product (r^2 = 0.57, P = 0.001). The stress value corresponds to disagreement between the two-dimensional configuration and predicted values, with stress <0.2 considered a good representation. Triplicates are plotted for all conditions except for crude oil treatment "Ambient 0.1%," for which one replicate was lost. Twelve microcosms were assessed to obtain day 0 (pre-treatment) microbial community data. Associated ANOSIM statistics and simper results are presented in Data Set S2. (B) Shannon Index (i.e., α-diversity) for each treatment group, with the central band representing the median among replicates, the box containing 50% of observations, and whiskers extending to the lowest and highest values excluding outliers (separate points). Aside from the pre-treatment box all treatments have two pairs, the first being the day 28 results, and the second being that of day 71.

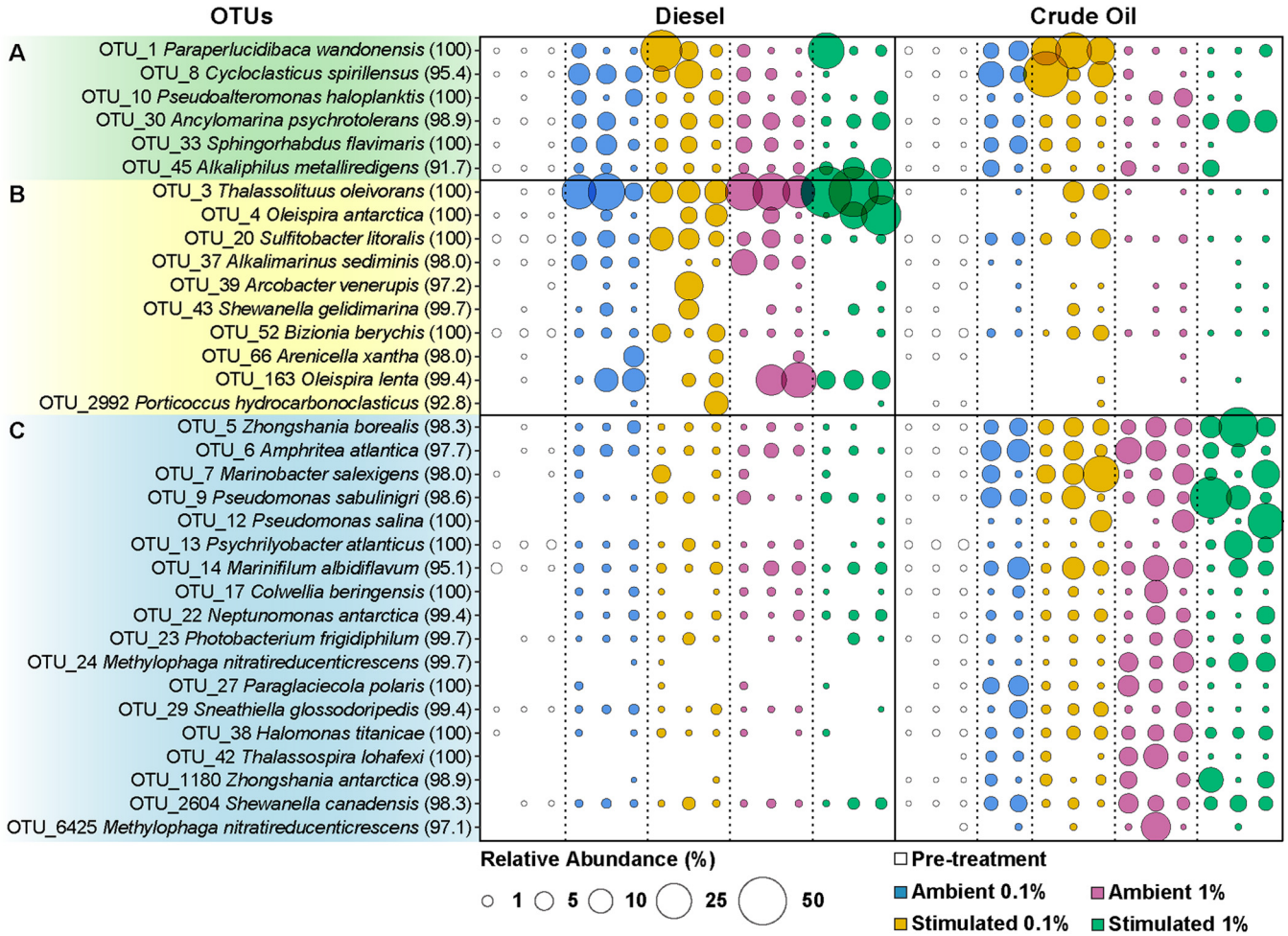

FIG 4 Relative sequence abundance of OTUs with significant associations to diesel or crude oil input after 71 days of incubation at 4°C. Bubble size indicates OTU relative abundance (%), with missing bubbles indicating no sequence reads. OTUs are labeled according to closest cultured relatives identified following NCBI BLAST searching with sequence identities (%) shown in parentheses. OTUs are grouped according to significant associations identified by "indicspecies" as those strongly correlated with both diesel and crude oil contamination (A), those correlated with the presence of diesel only (B), or crude oil only (C).

yields in DNA concentration (see Fig. S4), consistent with low temperature growth of a limited number of taxa in the presence of hydrocarbons.

Microbial response to hydrocarbon input and biostimulation at 4°C. Microbial groups affiliated to known aliphatic and aromatic hydrocarbon degrading taxa, originally at low levels at day 0, became abundant after 28 and 71 days of 4°C incubation in the presence of diesel or crude oil. Among 56 OTUs found to contribute to at least 50% of the dissimilarity between all groups tested using analysis of similarities (ANOSIM) (see Fig. S5 and Data Set S3), 34 were significantly associated with diesel and/or crude oil amendments (Fig. 4; see also Data Set S4). Of these OTUs, six were significantly associated with both diesel and crude oil amendments. Included in this group were *Paraperlucidibaca* OTU_1 and *Cycloclasticus* OTU_8, both exhibiting increases in abundance mainly in the 0.1% amendments. Diesel was significantly correlated with 10 OTUs, including *Oleispira* OTUs 4 and 163 and *Thalassolituus* OTU_3 that exhibited the greatest increases in relative abundance. Crude oil amendment led to 18 OTUs that were selectively enriched, with *Zhongshania* OTU_5, *Marinobacter* OTU_7, and *Pseudomonas* OTUs 9 and 12 exhibiting the greatest increases in relative abundance.

Specific bacteria were found to be significantly associated with specific diesel or crude oil concentrations or nutrient biostimulation (Fig. 4; see also Data Set S4), in

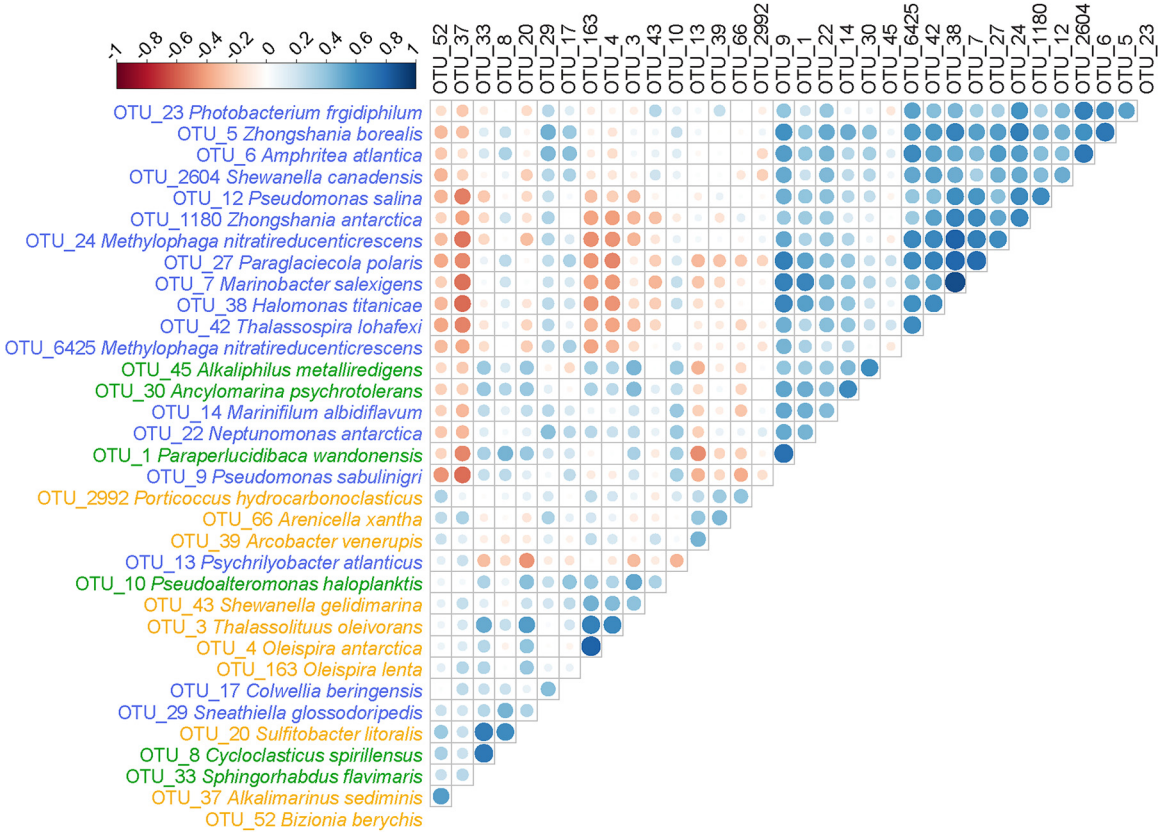

FIG 5 Spearman correlation matrix highlighting positive (blue) or negative (red) cooccurrence relationships between hydrocarbon associated OTUs (cross-reference with Data Set S4). Analysis utilized rarefied sequences from all incubations, both amended and unamended, at 0, 28, and 71 days of incubation. Empty boxes indicate no correlation was found between pairs, while the larger the circle size and darker the color, the stronger the correlation between associated OTUs. The highlighting of the OTUs indicates they were significant indicators of crude oil (blue), diesel (yellow), and both crude oil and diesel (green) enrichment.

some cases exhibiting strong cooccurrence with other OTUs (Fig. 5). In diesel-amended biostimulation treatments, *Oleispira* OTU_4 was significantly associated with 1% diesel, whereas *Porticoccus* OTU_2992 was prevalent only in 0.1% diesel, suggesting a differential affinity or tolerance for diesel between different taxa. Interestingly, the presence of *Cycloclasticus* OTU_8 was significant in all 0.1% diesel and crude oil amendments, suggesting broad affinity by this group but only at lower concentrations. Within crude oil amendments, *Marinobacter* OTU_7 was significantly associated with nutrient biostimulation, whereas *Colwellia* OTU_17 was only prevalent at the lower ambient nutrient condition, suggesting differential responses by putative oil-degrading bacteria to N and P addition. Diesel-associated *Oleispira* OTUs (4 and 163) shared a strong positive correlation with each other and with *Thalassolituus* OTU_3 (Fig. 5). These three diesel-associated OTUs exhibited strong negative correlations with many of the crude oil-associated OTUs, such as *Zhongshania* OTUs 5 and 1180, *Marinobacter* OTU_7, and *Pseudomonas* OTU_12.

Changes in microbial community composition reflect the response to hydrocarbons and biostimulation. Putative HCB, mostly belonging to the *Gammaproteobacteria*, increased in relative abundance within all diesel- and crude oil-amended microcosms (Fig. 6). Across all treatments, *Paraperlucidibaca* increased in relative sequence abundance from $<$0.1% before incubation to a maximum of 19% by day 28 and maintained a high relative abundance in many diesel- and crude oil-amended treatments at day 71 (Fig. 6A). *Cycloclasticus* increased in abundance from $<$0.08% to a maximum of 19%, increasing in all 0.1% diesel and 0.1% crude oil amendments until the end of the 71-day

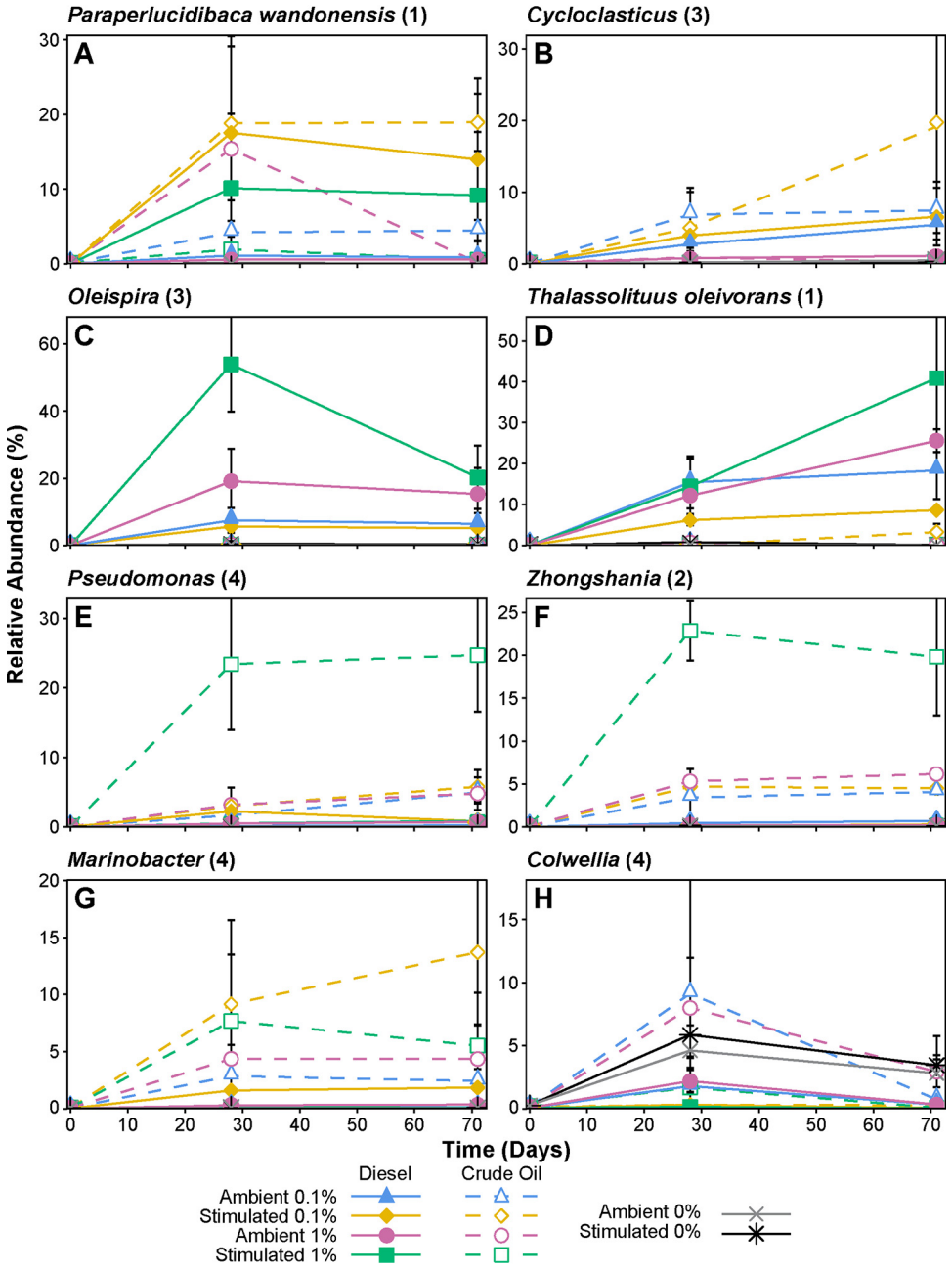

FIG 6 Relative sequence abundance of OTUs belonging to eight different genera, in response to amendment with different diesel and crude oil concentrations (0, 0.1, and 1% [vol/vol]), with (stimulated) or without (ambient) nutrient addition during 71 days of incubation at 4°C. The numbers of OTUs identified in this study belonging to each genus incorporated into the plotted data are shown in parentheses (*Paraperlucidibaca* and *Thalassolituus*, each containing only one OTU, include the closest cultured relatives according to NCBI BLAST searching). Error bars represent standard errors of triplicate microcosms of the same treatment.

incubation (Fig. 6B). Both *Oleispira* (<0.001% up to 54%; Fig. 6C) and *Thalassolituus* (<0.01% up to 41%; Fig. 6D) showed similarly large increases in relative sequence abundance but only in the presence of diesel. Whereas *Oleispira* declined in abundance after 28 days, *Thalassolituus* continued to increase in abundance between 28 and 71 days. Among bacteria responding to crude oil addition, *Zhongshania* (<0.06% up to 23%; Fig. 6F), *Marinobacter* (<0.04% up to 14%; Fig. 6G) and *Pseudomonas* (<0.04% up to 25%; Fig. 6E) showed the largest increases in relative abundance. None of these genera increased in abundance in unamended controls, whereas within the genus *Colwellia*

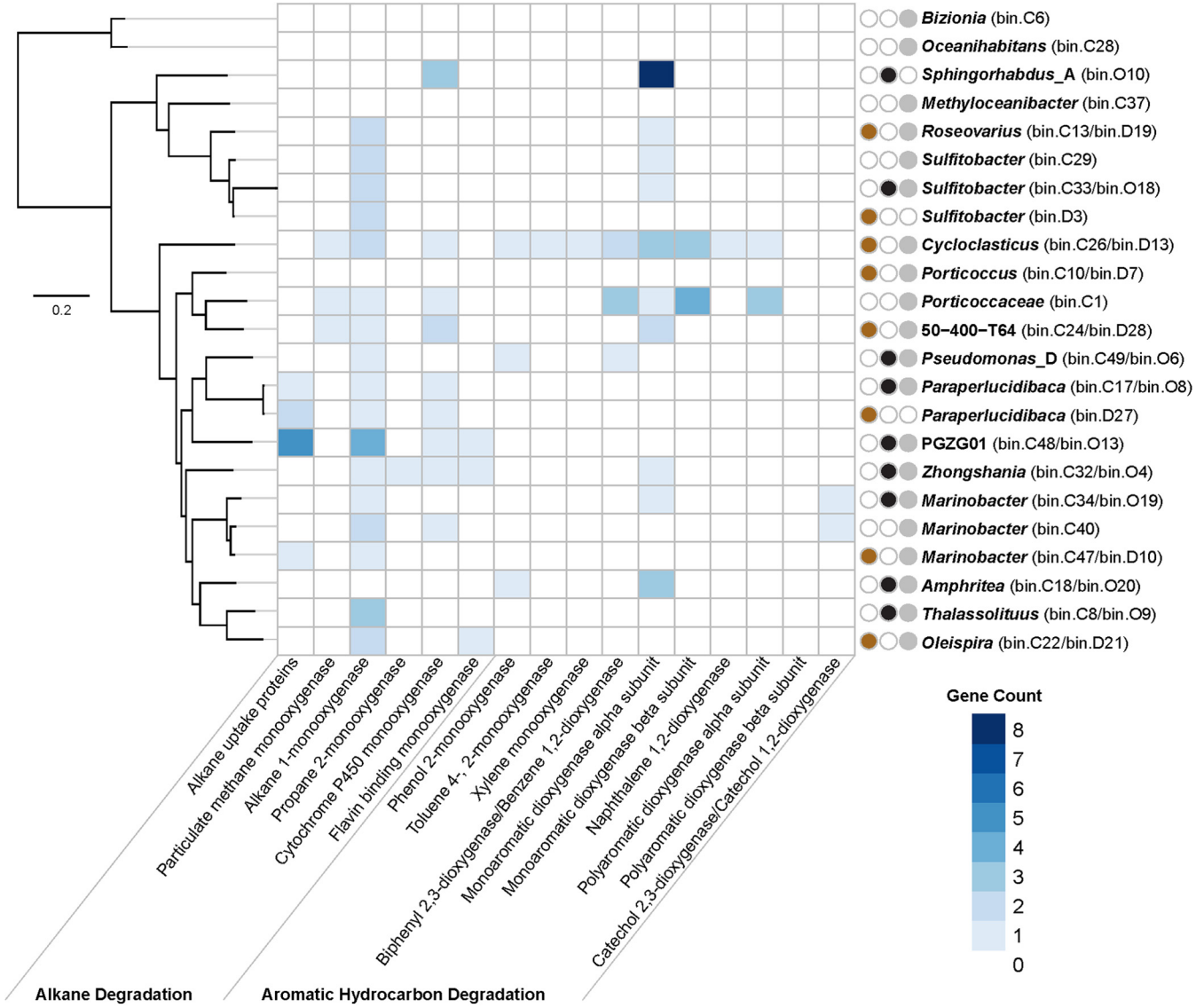

FIG 7 Heatmap representing the gene count of select biodegradation enzymes from MAGs recovered from metagenomic libraries constructed from microcosms amended with diesel (brown) or crude oil (black) and following coassembly of the two (gray). Bin names corresponding to these MAGs are indicated on the right (labeled D, O, and C, respectively) and are arranged according to a maximum-likelihood phylogenomic tree (shown at left) based on 43 concatenated marker genes. The scale bar indicates 0.2 substitutions per nucleotide position. Enzymes containing multiple subunits were counted once if all subunits were present (see Data Set S1). Unpaired mono- or polycyclic aromatic dioxygenase alpha and beta subunits were also counted.

some OTUs increased in some unamended controls, while others increased in crude oil-amended microcosms (Fig. 6H); *Colwellia beringensis* OTU_17 was enriched by crude oil amendment, whereas *Colwellia psychrerythraea* OTU_72 was only enriched among unamended controls (see Fig. S5).

Metagenome-assembled genomes (MAGs) with >70% completeness and <5% contamination were recovered (see Data Set S1) from diesel-amended microcosms (n = 8) and crude oil-amended microcosms (n = 9). Additional MAGs were also retrieved by coassembly of metagenomes from both conditions (n = 20). In total 37 MAGs were retrieved resulting in 23 unique genomes following the removal of duplicates generated by individual and coassemblies (Fig. 7). Enzymes of interest, including monooxygenases, ring-cleaving dioxygenases involved in aerobic activation of alkanes, and mono- or polycyclic aromatic hydrocarbons (40–43), were identified in all 37 MAGs (including duplicates). These metabolic capabilities are intrinsic to aerobic hydrocarbon biodegradation. Complete hydrocarbon degradation pathways among individual

genomes do not necessarily confirm the potential ecological effect of a given compound being fully degraded, and full degradation pathways may be shared among complex communities of microbes (44). For this reason, genes associated with initial activation of hydrocarbon degradation were analyzed for this study. Alkane uptake proteins (45) and catechol dioxygenases (46) were also investigated. Genes involved in hydrocarbon degradation were identified in 19 of the 23 unique MAGs (except *Bizionia*, *Oceanihabitans*, *Methyloceanibacter*, and *Porticoccus*; Fig. 7), consistent with hydrocarbon biodegradation potential being a prevalent phenotype among the microbial groups enriched by diesel and crude oil (Fig. 4 and 6). It is interesting that *Porticoccus* MAGs (>98% complete) lacked genes for hydrocarbon degradation, given that members of this genus are believed to degrade hydrocarbons in the phycosphere (47–49).

Alkane 1-monooxygenase genes were widespread among the majority of MAGs, further revealing the potential for alkane degradation in the Labrador Shelf sediment microbiome. This includes *Cycloclasticus*, which is shown here to harbor the potential for degradation of higher alkanes (Fig. 7). MAGs classified as *Paraperlucidibaca*, PGZG01, *Zhongshania*, *Thalassolituus*, and *Oleispira* are also capable of alkane degradation. While aromatic hydrocarbon degradation genes were less prevalent overall, they were abundant in *Cycloclasticus* and *Porticoccaceae* MAGs. *Pseudomonas*_D, *Marinobacter psychrophilus*, and *Amphritea* MAGs from crude oil amendments also have potential to degrade aromatic hydrocarbons (Fig. 7), consistent with the significantly higher losses of PAHs from these treatments compared to diesel amendments (Fig. 2C and D) and with previous reports of aromatic hydrocarbon biodegradation by *Amphritea* (50–52). MAGs with novel classifications in the Genome Taxonomy Database (GTDB) exhibiting hydrocarbon biodegradation potential included *Sphingorhabdus*_A, 50-400-T64, *Pseudomonas*_D, and PGZG01 (Fig. 7). Most of the MAGs did not include 16S rRNA genes, as has been observed by others (53), but bear taxonomic resemblance to the dominant OTUs that were identified by amplicon sequencing (Fig. 4).

DISCUSSION

Diesel and crude oil provoke different members of the Labrador Sea microbiome. Increases in the relative sequence abundance of key microbial taxa can highlight community succession in response to petroleum contamination. Several taxa showed dramatic increases in relative abundance in response to diesel or crude oil (Fig. 3A, 4, and 6), consistent with Baas Becking's principle that "everything is everywhere, but, the environment selects" (54). Comparisons revealed 10 OTUs specific to diesel and 18 OTUs specific to crude oil (Fig. 4). Among the six additional indicator OTUs that are shared between the two groups, the most prominent belonged to the *Gammaproteobacteria* and is closely related to *Paraperlucidibaca wandonensis* (100% sequence identity with OTU_1; Fig. 4A). Other than one study showing that *P. wandonensis* grown at 25°C can degrade Tween (55) (an oleophilic component of dispersants with moieties structurally similar to saturated hydrocarbons), little is known regarding the hydrocarbon degradation capability of *Paraperlucidibaca* spp. In agreement with the prominence of *Paraperlucidibaca* OTU_1 in both diesel- and crude oil-amended microcosms (Fig. 4), *Paraperlucidibaca* MAGs with high completeness (90 to 93%) were recovered from both metagenomic libraries and the coassembly (O8, D27, and C17; Fig. 7). All three MAGs shared >99.7% average nucleotide identity (ANI), indicating the same population was enriched by diesel and crude oil (Fig. 7). The only published *Paraperlucidibaca* genome (*P. baekdonensis*; GCA_003387535.1) shares ~81% ANI with these MAGs, demonstrating that the Labrador Sea *Paraperlucidibaca* is a separate clade that expands the genomic diversity of this genus. These MAGs contained alkane 1-monooxygenase and cytochrome P450 monooxygenase genes involved in alkane activation, as well as genes encoding uptake proteins that facilitate alkane transfer to the inside of the cell (45), whereas enzymes involved in aromatic hydrocarbon biodegradation were not detected (Fig. 7). This is consistent with *Paraperlucidibaca* being involved in the degradation of alkanes in

diesel and crude oil, resulting in its dramatic enrichment, most notably in the presence of nutrients (Fig. 4 and 6). The genus *Paraperlucidibaca* was proposed in 2011 for isolates with lower temperature optima than *Perlucidibaca* spp. (56). Results presented here suggest *Paraperlucidibaca* spp. also include previously unrecognized capabilities for low temperature alkane biodegradation.

Relatives of *Cycloclasticus spirillensus* (95.4% sequence identity with OTU_8; Fig. 4A) were also enriched in both diesel and crude oil amendments (Fig. 6). Unlike *Paraperlucidibaca*, members of the genus *Cycloclasticus* are well-known HCB (19, 57). *Cycloclasticus* MAGs were retrieved from diesel-amended microcosms and exhibited broad potential for hydrocarbon degradation with genes involved in metabolizing aromatic and aliphatic hydrocarbons (Fig. 7). Whereas the former is well known in *Cycloclasticus* (58), members of this genus were only recently shown to be able to degrade alkanes (59, 60). The MAGs obtained here share 76% ANI with *Cycloclasticus* strain TK-8 (confirmed as *Cycloclasticus pugetii*; https://bacdive.dsmz.de/) isolated from oil slicks of the DWH spill and found capable of degrading aliphatic hydrocarbons (specifically nC_{14} and nC_{15}) in Macondo oil (60). Similarly, these MAGs share 75% ANI with *Cycloclasticus* enriched from a temperate (6 to 8°C) marine channel on dilbit (a mixture of light and heavy petroleum compounds) that contains *alkB* (alkane hydroxylase responsible for aerobic alkane degradation) and *ladA* (a key gene specific to long-chain alkane degradation) (61). Duplicate *Cycloclasticus* MAGs (C26 and D13, 99.9% ANI; Fig. 7) from the Labrador Sea harbor genes for initiating the degradation of short-chain alkanes (e.g., particulate methane monooxygenase genes likely involved in fixing carbon derived from C_2–C_4 alkanes [59]; Fig. 7) and long-chain alkanes (e.g., alkane and cytochrome p450 monooxygenase genes; Fig. 7).

Compared against all published *Cycloclasticus* genomes, the highest match for these MAGs shares 89.4% ANI (*Cycloclasticus* sp002292375 and GCA_002292375.1), thus indicating a separate clade and further revealing the prevalence of alkane degradation within the genus. All alkane 1-monooxygenease genes from *Cycloclasticus* MAGs were compared between this study and that of Schreiber et al. (61), revealing a maximum amino acid identity of 77%. Not only is the potential to degrade alkanes broad among different *Cycloclasticus* spp., but these genes are also genetically diverse within the genus. *Cycloclasticus* may play a larger role in the degradation of alkanes in the marine environment than previously thought, an important consideration given that gaseous and other alkanes are released from natural hydrocarbon seeps (62, 63) and from spills like the DWH (64–66) where *Cycloclasticus* was heavily enriched (67). Whether *Cycloclasticus* were responsible for higher alkane degradation in the Labrador Sea microcosms is not clear, given that many other alkane degraders were also present (Fig. 7). On the other hand, of the 23 unique MAGs recovered, *Cycloclasticus*, along with *Porticoccaceae*, encoded the most extensive suite of aromatic hydrocarbon biodegradation genes, with 10 other MAGs exhibiting potential to degrade these compounds to a lesser degree (Fig. 7). The enrichment pattern and genomics of cold-adapted *Cycloclasticus* in the Labrador Sea provide additional evidence that members of this genus are versatile hydrocarbon degraders in low temperature marine environments.

The microbial response specific to diesel amendment (Fig. 4B) featured enrichment of *Oceanospirillales* closely related to *Oleispira antarctica* (100% sequence identity with OTU_4), *Oleispira lenta* (99.4% sequence identity with OTU_163) and *Thalassolituus oleivorans* (100% sequence identity with OTU_3). These genera are known to encompass alkane degraders (68–71) and were especially prevalent in 1% diesel-amended microcosms (Fig. 6C and D), where extensive mineralization (Fig. 2E) was driven primarily by alkane degradation (Fig. 2A and C). *Oleispira* spp. include psychrophiles that respond to oil inputs in cold marine settings (72), possibly explaining *Oleispira* responding rapidly to alkanes in diesel at 4°C, followed by *Thalassolituus* (Fig. 6C and D). These and other *Oceanospirillales* lineages were shown to dominate the microbiome within the crude oil plume during the first month of the Deepwater Horizon oil spill (22, 23, 73) (n.b., many of these groups are reclassified as *Pseudomonadales* in the GTDB [74, 75]).

MAGs classified as *Oleispira antarctica* and *Thalassolituus oleivorans* both include multiple genes encoding alkane 1-monooxygenase (Fig. 7). *Oleispira* and *Thalassolituus* OTUs were much less prevalent in the presence of crude oil (Fig. 4C and Fig. 6C and D), which experienced less alkane biodegradation than diesel (Fig. 2A to D).

Relatives of *Zhongshania borealis* (98.3% sequence identity with OTU_5) and *Zhongshania antarctica* (98.9% sequence identity with OTU_1180) (Fig. 4C) were enriched only in the presence of crude oil, two organisms not previously known to degrade hydrocarbons. *Zhongshania* MAGs recovered from crude oil-amended microcosms harbor a suite of alkane degradation, as well as some monoaromatic dioxygenase genes (Fig. 7). *Zhongshania* spp. more distantly related to OTU_5 and OTU_1180 have been shown to degrade aliphatic hydrocarbons (i.e., *Z. aliphaticivorans*) (76) and *Zhongshania* genomes detected in other cold marine oil bioremediation studies show similar genetic potential for alkane and aromatic hydrocarbon degradation (77, 78) as the MAGs from the Labrador Sea (Fig. 7). This potential and the ubiquity of *Zhongshania* in polar regions (76, 79, 80) suggests this lineage may be relevant as an indicator of hydrocarbon biodegradation during monitored natural attenuation of oil spills in cold marine environments. MAGs classified by GTDB-Tk as PGZG01, within the family *Alcanivoracaceae*, were also retrieved from the 0.1% crude oil amendments. The PGZG01 group may correspond to a novel genus with high potential for low temperature marine alkane degradation, as evidenced by four genes for alkane 1-monooxygenase and five pairs of genes encoding alkane uptake proteins (Fig. 7). An interesting observation in the sediment incubations conducted here is that *Zhongshania* and PGZG01, together with *Paraperlucidibaca*, likely contributed to the biodegradation of alkanes from crude oil by outcompeting well-known *Oleispira* and *Thalassolituus* at 4°C. Understanding subtle differences in microbial responses to diesel and crude oil is a necessary precursor for several bioremediation strategies (81) and will help inform effective responses to future spills.

Biostimulation promotes biodegradation and microbial community turnover at 4°C. Naturally low concentrations of nitrogen and phosphorus in the marine environment combined with low temperatures in regions like the Labrador Sea are constraints governing the biodegradation of spilled hydrocarbons. This study showed how diesel and crude oil spills in concentrations of 0.1 and 1% (vol/vol) rapidly deplete the ambient nutrient supply (see Fig. S2), thereby limiting the extent of biodegradation that is possible. As a marine oil spill response measure, biostimulation is considered worthwhile if the biodegradation rate can be doubled (82). Nutrient application resulted in respiration rates that more than doubled during the first few weeks of incubation (Fig. 2G and H), coinciding with accelerated removal of alkanes and PAHs (Fig. 2C and D). Respiration rates coupled to diesel and crude oil degradation declined after the first 28 days of 4°C incubation (Fig. 2G and H). It has been suggested that nutrient biostimulation may be most effective early on, as observed here, and that following an initial pulse of activity in response to nutrient addition, natural attenuation without additional biostimulation may be a preferable strategy (83, 84).

Different genera were enriched in response to different diesel and/or crude oil treatments, with or without nutrient stimulation (Fig. 4 and 6). Shifts in microbial community composition and α-diversity (Fig. 3) are consistent with other studies showing that oil contamination facilitates growth and competition leading to less diverse communities (21, 77, 78, 85). Sun et al. (86) reported that microbial communities stimulated with 2% (wt/vol) crude oil, much higher nutrient concentrations, and incubated at 30°C were not significantly different from those treated with oil alone; nutrients influenced the succession of bacterial communities, while actual differences were more closely related to the addition of crude oil. In this more realistic marine oil spill scenario using Labrador Sea sediments incubated at cold *in situ* temperature, comparing ambient and biostimulated nutrient treatments showed that nutrient addition similarly influences community succession and timing whereas responding populations were influenced more by the petroleum product. Major community shifts in response to biostimulation occurred within the first 28 days when rates of CO_2 generation were greatest (Fig. 2E and F). Nutrient stimulated treatments exhibited the most significant

change in Bray-Curtis dissimilarity during this period (Fig. 3A; see also Data Set S3) and potentially allowed HCB to establish earlier as evidenced by the shorter apparent lag in respiration among diesel amendments (Fig. 2E).

Biostimulation enhanced the loss of hydrocarbons in 0.1% diesel and crude oil amendments (Fig. 2A to D) but had almost no effect in the presence of 1% diesel or crude oil, with the exception of alkanes in diesel being consumed (Fig. 2A). Greater alkane losses and CO_2 production (Fig. 2E and F) coupled with low PAH losses among nutrient-stimulated 1% diesel treatments were likely due to a large bloom in biomass (as evidenced by DNA yields; see Fig. S4) consisting of alkane-degrading bacteria (i.e., *Thalassolituus*, *Oleispira*, and *Paraperlucidibaca*; Fig. 4) and a lack of succession to aromatic hydrocarbon degraders (21). *Cycloclasticus* (OTU_8) was one of the only OTUs with corresponding potential for aromatic hydrocarbon biodegradation (Fig. 7) to be enriched in the presence of diesel, but its low abundance in 1% diesel amendments by day 71 suggests community succession did not occur (Fig. 4A). This points to the concentration of spilled petroleum playing a role in the timing of community succession even when nutrients are not limiting. Among 1% crude oil amendments there was no difference in alkane or PAH losses between ambient nutrient and stimulated treatments, despite large increases in CO_2 in the latter (Fig. 2E and F). Compounds other than the measured alkanes and PAHs may account for this activity, and it cannot be ruled out that increases in CO_2 in these nutrient-stimulated crude oil microcosms (Fig. 2F) are due to degradation of necromass owing to toxicity that 1% crude oil exerts on the community as a whole. Toxic components of crude oil that are not present in diesel may include certain monoaromatics, *n*-alkanols, and terpenoids (87), potentially explaining these results. High levels of certain compounds may strongly inhibit bacterial growth, resulting in poor biodegradation efficiency (88, 89), potentially rendering nutrient addition ineffective among 1% crude oil treatments.

Whether biostimulation should be used in response to spilled hydrocarbons will be situationally dependent, determined by the environment, the type of petroleum product released, and its volume and concentration. Nutrient application along shorelines after the Exxon Valdez oil spill proved successful at enhancing biodegradation (9, 84, 90, 91). Areas of upwelling or terrestrial runoff where nutrient concentrations may be naturally elevated could further mitigate hydrocarbon pollutants in the event of a spill, and such areas should be identified when planning shipping routes through remote environments. Whereas chemical dispersants are used in response to oil spills in open water (92) where biostimulation would result in rapid dilution of applied nutrients, dispersants will have limited effectiveness in instances where physical factors result in pooling of the petroleum contamination. The concentrations of diesel and crude oil employed in the low-temperature Labrador Sea sediment experiments presented here are higher than what would be encountered following dispersant application in open water (28) and are more realistic in the context of pooling associated with shorelines (9, 84), sea ice floes (93), or upon export to the seabed via sedimentation and accumulation (94–96). Residual hydrocarbons in Gulf of Mexico sediments in the aftermath of the DWH spill were greater than 100 ppm and represent a continuing issue due to long-term persistence and potential redistribution (97). Biostimulation technologies that target hydrocarbons in sea-floor sediments may prevent prolonged exposure of benthic organisms such as economically important fish in the Gulf of Mexico or those essential to the traditional livelihoods of communities along the coast of the Labrador Sea. This study demonstrates the potential for low-temperature biodegradation by Labrador Sea microbial communities and the likelihood for nutrient biostimulation to enhance this response.

MATERIALS AND METHODS

Labrador Shelf sediment collection. Sediment samples were collected in 2015 aboard the Canadian Coast Guard Icebreaker *Amundsen* at 58°55.609N, 62°09.326W in the Labrador Sea (Fig. 1) from water depths ranging from 141 to 145 m (see Table S1). Surface sediment was collected from within the top 0 to 5 cm of three separate box core casts (see Table S1) and immediately stored in sterile plastic

bags at 4°C on board the ship. Upon return to the University of Calgary, bulk sediments remained stored at 4°C for several months until microcosms were established.

Hydrocarbon- and nutrient-amended microcosm incubations at 4°C. Triplicate microcosms were established from separate sediment samples from the triplicate box core casts. Diesel used in this experiment was obtained from a local gas station where common diesel is comprised of 75% saturated hydrocarbons and 25% aromatic hydrocarbons with an average formula of $C_{12}H_{23}$. Crude oil used in this experiment came from the Macondo oil reservoir in the Gulf of Mexico, and similar to crude oils produced offshore Newfoundland and Labrador, is a light, nonviscous oil with initial API gravity of 35° (98). Microcosms were established in 160-ml glass serum bottles with a 1:4 ratio of sediment to medium and incubated at 4°C to simulate ambient benthic temperatures. Artificial seawater (ASW) medium (99) was added as 40 ml except for the sediment-free control bottles which had the sediment volume replaced by using 50 ml of medium. Sodium sulfide was omitted from the ASW to promote oxic conditions in the microcosms. All bottles were hermetically sealed and a slight overpressure was established using filter-sterilized (0.2 μm) air. For diesel amendments, despite adding 20-ml sterilized air to provide ample oxygen for the duration of the experiment, one treatment group (nutrient stimulated 1% [vol/vol] diesel, all three replicates) became anoxic (see Fig. S1E). The initial volume of injected air for subsequent crude oil amendments was therefore increased to 60 ml to prevent the establishment of anoxic conditions (see Fig. S1F).

Four treatment groups were established for both diesel and crude oil amendments using two batches of ASW, one with a low level of N and P (15 μM NH_4Cl and 2 μM KH_2PO_4) to mimic regional bottom water concentrations (100), and one with higher levels (4.67 mM NH_4Cl and 1.47 mM KH_2PO_4), to simulate nutrient biostimulation. The lower concentrations were selected to observe how rapidly ambient nutrient levels deplete after the introduction of hydrocarbons, thus impacting rates of hydrocarbon biodegradation. The higher nutrient concentrations satisfy the Redfield ratio by providing much more N and P than would be required to degrade the volumes of diesel and crude oil added in order to demonstrate how nutrient addition can further stimulate hydrocarbon degradation. Either diesel or crude oil was added at concentrations of 0.1 or 1.0% (vol/vol) of the combined sediment and medium (i.e., 50 or 500 μl, respectively). These levels were selected to determine whether concentration influenced microbial community composition and response, with 1% representing a pooled oil scenario and 0.1% representing a more dispersed scenario. Densities of Macondo crude oil and diesel are 0.84 and 0.85 g/cm^3, respectively; thus, their concentration per gram of wet sediment in incubations was estimated at 840 to 860 μg g^{-1} in 0.1% (vol/vol) incubations, and 8,400 to 8,600 μg g^{-1} in 1% (vol/vol) incubations. For each diesel or crude oil concentration, a parallel set of microcosms was prepared and immediately frozen at −20°C for chemical analyses of hydrocarbons to define preincubation conditions. The experimental setup included sediment-free controls, killed (autoclaved) controls, and unamended (i.e., no diesel or crude oil) controls. Killed controls were autoclaved once at the onset of the diesel experiment, and three times at the onset of the crude oil experiment. All microcosms were incubated at 4°C and monitored for 71 days.

Gas chromatography measurements. Concentrations of CO_2 and O_2 in all microcosms were monitored at 0, 11, 28, and 71 days by injecting 1 ml of headspace gas into an Agilent 7890B gas chromatograph (GC). Separation of CO_2 was performed on a GC packed Hayesep N packing column (stainless steel tubing, 0.5-m length × 1/8″ OD, 2-mm internal diameter [ID]; mesh size, 80/100), followed by a similar column at 1.83-m length. Separation of O_2 was performed on a GC packed MolSieve 5A packing column (UltiMetal tubing, 2.44 m, 1/8″ OD, 2-mm ID; mesh size, 60/80). Helium was applied as the carrier gas at a flow rate of 21 ml/min. Gases were detected by a thermal conductivity detector (TCD-3) set to 200°C. The oven temperature program was set to 105°C for 5 min.

Hydrocarbon analysis by gas chromatography-mass spectrometry. Hydrocarbons were extracted from diesel- and crude oil-amended microcosms that had been frozen at −20°C after the 71-day incubation period, as well as from duplicate treatment microcosms immediately frozen at day 0. After thawing, hydrocarbons were extracted via dissolution in dichloromethane (DCM) with the use of sonication. Extracts were run through a column of sodium sulfate to remove any residual water, and DCM was evaporated to a final concentrated volume of 1 ml. Extracts were injected for GC-MS using an Agilent 7890B GC and 5977A quadrupole mass-selective detector. Samples were injected as a 1 μl aliquot and separation was performed on a HP-5 MS capillary column (Agilent, 30 m × 0.25-mm ID × 0.25-μm film thickness) with a splitless injector (pulsed mode) at 250°C. High-purity helium (99.999%) was applied as the carrier gas at a flow rate of 1 ml/min. The temperature program was as follows: 40°C held for 5 min, followed by heating to 325°C at 4°C/min and finished with an isothermal hold for 15 min at 325°C. The mass spectrometer acquired data in a combined full scan/selected ion monitoring (SIM-SCAN) mode. An ion abundance of 500,000 to 1,000,000 was required; therefore, certain samples were concentrated or diluted with DCM to fit that range and rerun. Using Agilent MSD ChemStation E.02.02.1431, alkane (*n*-alkanes C_{12}-C_{25} and pristane), and PAH (phenanthrene, biphenyl, naphthalene, methylnaphthalene (MN; 1-MN and 2-MN), dimethylnaphthalene (DMN; 2,6+2,7-, 1,3+1,7-; 1,6-; 1,4+2,3-; and 1,5-DMN), and trimethylnaphthalene (TMN; 1,3,7-, 1,3,6-, 1,2,4-, 1,2,5-, and 1,2,3-TMN) fragments were identified and ion peaks integrated. GC-MS measurements were used as a metric to assess degradation between the different treatment conditions, with the same compounds compared following amendment with diesel or crude oil.

Identification of conserved markers for determining biodegradation. Common diagnostic isomer ratios (see Table S2) were used for confirmation of both alkane (*n*-C_{17}/pristane) (101), and PAH (2-methylphenanthrene/1-methylphenanthrene) (102) degradation. Biodegradation was further determined as the preferential loss of select compounds compared against chemical constituents understood

to be recalcitrant to degradation, described below. Depletion of target compounds in diesel or crude oil was calculated using the following equation (103), where A_s and C_s are the concentrations of the target compound and conserved compound in the 71-day incubation, respectively, and A_0 and C_0 are the concentrations at day 0:

$$\%\,\text{loss} = [((A_0/C_0) - (A_s/C_s))/(A_0/C_0)] \times 100$$

In crude oil-amended samples, integrated areas were normalized against the area of the conserved compound C_{30}-hopane [17α(H),21β(H)-hopane]. Hopanes are common among crude oils and very resistant to biodegradation making them an ideal internal standard for assessing the biodegradation of other oil compounds (104). Since hopanes are not present in diesel, 1,3+3,9+2,10+3,10-dimethylphenanthrene was used as the conserved compound for normalization to assess biodegradation in diesel-amended microcosms. Methylated phenanthrenes have previously been used as conserved markers in the biodegradation of diesel (105).

16S rRNA gene amplicon sequencing and analysis. DNA was extracted from frozen microcosm sediment slurry samples taken at days 0, 28, and 71 using the Qiagen DNeasy PowerLyzer PowerSoil kit and manufacturer instructions. Immediately prior to bead beating, 300-μl samples were heated to 70°C for 10 min to assist with cell lysis. The PowerLyzer 24 bead beater was operated at 6,000 rpm for 40 s. At the final extraction step, 50 μl of elution buffer heated to 50°C was used. Extracted DNA was quantified using a Qubit fluorometer and stored at −20°C. For each round of DNA extraction, one procedural blank consisting of 300 μl extraction buffer was included. PCR of 16S rRNA genes used Illumina modified primers 341F (S-*-Univ-0341-b-S-17) and 806R (S-d-Bact-0787-b-A-20), as described elsewhere (106, 107), in 25-μl reactions (contents: 12.5 μl of 2× KAPA HiFi Hot Start Ready Mix, 2.5 μl of each primer [1 mM], 1 to 10 μl of template DNA, and sterile water). Using an Eppendorf thermal cycler the double-stranded DNA was denatured at 95°C for 3 min, followed by 25 cycles of denaturation at 95°C for 30 s, annealing at 56°C for 45 s, extension at 72°C for 1 min, and then a final extension at 72°C for 5 min. PCR products were run on a 1% agarose gel stained with SYBR green (Thermo Fisher Scientific) to confirm amplicons of the expected length and no amplicons in negative controls. For each sample, three separately amplified PCR products were pooled to reduce bias associated with early cycle PCR-induced errors and to minimize PCR drift (108). PCR products were purified using AMPure XP magnetic beads, barcoded with Illumina index primers as described previously (109), quantified using the Qubit fluorometer, pooled by normalizing for the concentration of DNA among samples, then sequenced using an in-house Illumina MiSeq (Energy Bioengineering and Geomicrobiology group, University of Calgary). Pooled libraries were sequenced using a 600 cycle MiSeq v3 reagent kit, producing 2 × 300-bp paired-end reads.

Sequence files (FASTA) were uploaded and analyzed using MetaAmp version 2.0 (110), a pipeline for processing of SSU rRNA genes using UPARSE, Mothur, and the SILVA database. Parameters were set to assemble pair-end reads and cluster them into OTUs according to a 97% sequence identity cutoff. The minimum length overlap of pair end reads was selected as 80 bp, with a maximum of 8 bp (10%) mismatches allowed in the overlap region. Default quality filtering options were used (maximum number of differences to the primer sequence, 0; maximum number of expected errors, 1; trimmed amplicon length, 350). The generated OTUs were given taxonomic assignments by MetaAmp via sequence comparisons with the SILVA database. Prokaryotic 16S rRNA genes and that of chloroplasts are homologous; therefore, amplified chloroplast 16S rRNA genes were removed from these files to allow for microbial analysis exclusively.

Metagenomic sequencing and analysis. Triplicate DNA extractions were pooled from nutrient stimulated microcosms incubated for 71 days with 0.1% (vol/vol) diesel or crude oil. DNA was mechanically sheared using a Covaris S220 Focused-ultrasonicator (Covaris, Inc., Woburn, MA) to generate ~450-bp fragments. Libraries were constructed using the NEBNext Ultra II Library Prep kit (New England Biolabs, Inc., Ipswich, MA) and sequenced on an Illumina NovaSeq S4 (PE 150 × 150; Illumina, Inc., San Diego, CA) at the Center for Health Genomics and Informatics, University of Calgary. Quality filtering of raw paired-end reads was performed using BBDuk with the parameters *qtrim = rl trimq = 20 minlength = 30 entropy = 0.5* (http://jgi.doe.gov/data-and-tools/bb-tools/) to remove Illumina adapters, phiX sequences, and reads shorter than 30 bp. Post-QC read quality was evaluated using FastQC (http://www.bioinformatics.babraham.ac.uk/projects/fastqc/). Resulting metagenome libraries for diesel- and crude oil-amended incubations were 30.1 and 31.8 million paired-end reads, respectively.

Libraries were assembled individually and coassembled using MEGAHIT v1.2.2 (111) with the parameters *-min-contig-len 500* to ensure contigs longer than 500 bp. Quality filtered reads were mapped to both assemblies and the coassembly using BBMap with default parameters. This was followed by generation of sequencing depth profiles using the *jgi_summarize_bam_contig_depths* tool provided with MetaBAT2 (112), which provided differential coverage values to improve binning. Metagenome-assembled genomes (MAGs) were binned using MetaBAT2 with default parameters and then evaluated for completeness and contamination using the *lineage_wf* workflow of CheckM v1.0.11 (113). MAGs were assigned taxonomy using the *classify_wf* workflow of GTDB-Tk v1.3.3 (114). The marker gene concatenated alignment of the selected MAGs generated by CheckM was used to construct a phylogenomic tree using FastTree v2.1.5 (115). To assess the presence of hydrocarbon degradation genes and pathways, a comprehensive annotation profile for each assembly was generated using MetaErg (116) with parameters *–mincontiglen 500 –minorflen 180 –gtype meta –gcode 11*. The annotation profile contains the prediction and abundances of protein-coding genes. Proteins of interest identified from MetaErg outputs were verified using NCBI Protein BLAST (117) and presented in Data Set S1. Duplicate MAGs were obtained by running individual assembly and coassemblies. Instead of eliminating duplicates with

dereplication, both were investigated for protein-coding genes owing to some duplicates having different levels of completeness. FastANI (118), with minimum fragment length set to 1,000 bp and other parameters set to default, was used to compare the percent average nucleotide identity (ANI) of select MAGs and published genomes. To identify potential contamination in contigs from select MAGs (*Cycloclasticus*, *Paraperlucidibaca*, and *Zhongshania*), MAGPurify (119) modules "gc-content" and "tetra-freq" were run to identify any contigs with outlier nucleotide composition based on GC content and tetranucleotide frequencies, respectively. No contamination was found among the investigated genomes.

Data analysis. Data for gas values, hydrocarbon losses, and 16S rRNA gene comparisons were tested for significance using analysis of variance (ANOVA) and tested for normality using ANOVA residuals with the Shapiro-Wilk test (see Data Set S2). Significant ANOVAs were further analyzed with *post hoc* multiple pairwise comparisons using the Tukey HSD test. Non-normally distributed data (*P* value of Shapiro-Wilk normality test, <0.05) were analyzed using the Kruskal-Wallis rank sum test, followed by the pairwise Wilcox test. A *P* value of 0.05 was used as the cutoff for statistical significance. All statistical analyses were performed using R (120) and test results are presented in Data Set S2.

Microbial community analysis was performed in R using output files generated by MetaAmp 2.0 and R scripts available online (https://jkzorz.github.io/blog/). Community analyses comparing OTU or genus abundance between treatments were generated using full library sequence reads, ranging from 3,793 to 136,349 reads after chloroplast removal (see Table S3). Community analyses involving α- and β-diversity comparisons between treatments (NMDS, Shannon Index, and observed OTUs) used MetaAmp sequence data rarefied to the lowest library sequence value (i.e., 4,677). OTU correlations were performed using the Spearman's rank correlation coefficient. Bray-Curtis dissimilarity was used to quantify the differences between microbial communities of treatment and control groups based on 16S rRNA gene libraries and visualized using NMDS implemented by the R package "vegan" (121) to assess changes in community composition in response to hydrocarbon- and nutrient-amendment over time. The ANOSIM function in vegan was used to test for statistically significant differences between designated groups (see Data Set S3). The function "envfit" was used to plot experimental vectors and factors (nutrient concentration, petroleum product, and hydrocarbon concentration), their correlation with the ordination, and r^2 and significance values. The similarity percentage function "simper" (122) was used to identify the OTUs that contributed most to community dissimilarities identified through ANOSIM by performing pairwise comparisons of groups and finding the average contributions of each OTU to the average overall Bray-Curtis dissimilarity (see Data Set S3). OTUs that contributed to at least 50% of the dissimilarity were examined using the R package "indicspecies" (123) to determine those significantly associated with a given treatment (see Data Set S4). The taxonomy of key OTUs was determined by comparing the representative sequence with closest cultured relatives in the GenBank database following NCBI BLAST searching of the RNA reference database (117).

Data availability. All raw 16S rRNA gene sequence reads generated for this study have been submitted to NCBI's Sequence Read Archive (SRA) and are available within the BioProject PRJNA686385 (accession numbers SRX9713174 to SRX9713253). Raw metagenome sequence reads have been submitted to SRA (accession numbers SRX10509741 to SRX10509742), and MAGs have been submitted as a Whole Genome Shotgun (WGS) project (accession numbers JAGPUQ000000000 to JAGPWA000000000), all under the same BioProject.

SUPPLEMENTAL MATERIAL

Supplemental material is available online only.

SUPPLEMENTAL FILE 1, PDF file, 1 MB.

SUPPLEMENTAL FILE 2, XLSX file, 0.1 MB.

SUPPLEMENTAL FILE 3, XLSX file, 0.02 MB.

SUPPLEMENTAL FILE 4, XLSX file, 0.03 MB.

SUPPLEMENTAL FILE 5, XLSX file, 0.02 MB.

ACKNOWLEDGMENTS

This research was supported by funding awarded to C.R.J.H. by ArcticNet, Genome Canada, Genome Alberta, the Government of Alberta, and the MEOPAR network. S.M.C.M. was supported by scholarships provided by Alberta Innovates (Technology Futures Graduate Student Scholarship), The Association of Canadian Universities for Northern Studies and The W. Garfield Weston Foundation (Award for Northern Research), The Natural Sciences and Engineering Research Council of Canada (Graduate Scholarship), and the province of Alberta (Queen Elizabeth II Scholarship).

We thank Rhonda Clark for organizing field work and for research support, Jianwei Chen for assistance with gas chromatography, Carmen Li for performing Illumina MiSeq 16S rRNA gene sequencing, Srijak Bhatnagar for assistance with metagenomic sequencing, Xiaoli Dong for bioinformatics assistance, and Amy Noël for contributing to experimental design. We thank the PRG Laboratory, especially Kim Nightingale for performing gas chromatography-mass spectrometry on hydrocarbon extracts, and

Priyanthi Weerawardhena for method training. We thank The Gulf of Mexico Research Initiative and the C-IMAGE consortium for providing Macondo crude oil. We thank Anirban Chakraborty, Emil Ruff, and Jackie Zorz for their assistance with 16S rRNA analysis. We thank Jayne Rattray and Alastair Smith for their assistance with GC-MS analysis. We also thank Lisa Gieg, Roger Prince, and Steven Vamosi for their valuable discussions and input. The authors are grateful to the Canadian Coast Guard and specifically the crew of the CCGS *Amundsen* for their participation and assistance during field work.

We declare there are no conflicts of interest.

REFERENCES

1. Dawson J, Pizzolato L, Howell SE, Copland L, Johnston ME. 2018. Temporal and spatial patterns of ship traffic in the Canadian Arctic from 1990 to 2015. Arctic 71:15–26. https://doi.org/10.14430/arctic4698.
2. Lasserre F, Pelletier S. 2011. Polar super seaways? Maritime transport in the Arctic: an analysis of shipowners' intentions. J Transp Geogr 19:1465–1473. https://doi.org/10.1016/j.jtrangeo.2011.08.006.
3. Smith LC, Stephenson SR. 2013. New trans-Arctic shipping routes navigable by midcentury. Proc Natl Acad Sci U S A 110:E1191–E1195. https://doi.org/10.1073/pnas.1214212110.
4. Murphy D, Gemmell B, Vaccari L, Li C, Bacosa H, Evans M, Gemmell C, Harvey T, Jalali M, Niepa TH. 2016. An in-depth survey of the oil spill literature since 1968: long term trends and changes since Deepwater Horizon. Mar Pollut Bull 113:371–379. https://doi.org/10.1016/j.marpolbul.2016.10.028.
5. Arctic Monitoring and Assessment Programme. 2018. AMAP assessment 2018: biological effects of contaminants on arctic wildlife and fish. Working Group of the Arctic Council. https://www.amap.no/documents/doc/amap-assessment-2018-biological-effects-of-contaminants-on-arctic-wildlife-and-fish/1663.
6. Meredith M, Sommerkorn M, Cassotta S, Derksen C, Ekaykin A, Hollowed A, Kofinas G, Mackintosh A, Melbourne-Thomas J, Muelbert MMC, Ottersen G, Pritchard H, Schuur EAG. 2019. Polar regions. *In* IPCC Special Report on the ocean and cryosphere in a changing climate. Intergovernmental Panel on Climate Change. https://www.ipcc.ch/srocc/chapter/chapter-3-2/.
7. Barber DG, Babb DG, Ehn JK, Chan W, Matthes L, Dalman LA, Campbell Y, Harasyn ML, Firoozy N, Theriault N, Lukovich JV, Zagon T, Papakyriakou T, Capelle DW, Forest A, Gariepy A. 2018. Increasing mobility of high Arctic sea ice increases marine hazards off the east coast of Newfoundland. Geophys Res Lett 45:2370–2379. https://doi.org/10.1002/2017GL076587.
8. Sikumiut Environmental Management, Ltd. 2008. Strategic environmental assessment labrador shelf offshore area: final report. Sikumiut Environmental Management, Ltd, St. John's, Newfoundland, Canada. https://www.cnlopb.ca/sea/labrador/.
9. Atlas RM, Hazen TC. 2011. Oil biodegradation and bioremediation: a tale of the two worst spills in US history. Environ Sci Technol 45:6709–67145. https://doi.org/10.1021/es2013227.
10. Andrews J, Babb D, Barber D. 2018. Climate change and sea ice: shipping in Hudson Bay, Hudson Strait, and Foxe Basin (1980–2016), p 6–19. Elementa, Washington, DC.
11. Joye S. 2015. Deepwater Horizon, 5 years on. Science 349:592–593. https://doi.org/10.1126/science.aab4133.
12. Parmar TK, Rawtani D, Agrawal YK. 2016. Bioindicators: the natural indicator of environmental pollution. Front Life Sci 9:110–118. https://doi.org/10.1080/21553769.2016.1162753.
13. Leahy JG, Colwell RR. 1990. Microbial degradation of hydrocarbons in the environment. Microbiol Rev 54:305–315. https://doi.org/10.1128/mr.54.3.305-315.1990.
14. Lee K. 2000. *In situ* bioremediation of oiled shoreline environments, p 44–60. *In* Opportunities for environmental applications of marine biotechnology: workshop proceedings. National Academy Press, Washington, DC.
15. Crisafi F, Genovese M, Smedile F, Russo D, Catalfamo M, Yakimov M, Giuliano L, Denaro R. 2016. Bioremediation technologies for polluted seawater sampled after an oil-spill in Taranto Gulf (Italy): a comparison of biostimulation, bioaugmentation and use of a washing agent in microcosm studies. Mar Pollut Bull 106:119–126. https://doi.org/10.1016/j.marpolbul.2016.03.017.
16. Wilkinson J, Beegle-Krause CJ, Evers KU, Hughes N, Lewis A, Reed M, Wadhams P. 2017. Oil spill response capabilities and technologies for ice-covered Arctic marine waters: a review of recent developments and established practices. Ambio 46:423–441. https://doi.org/10.1007/s13280-017-0958-y.
17. Joye S, Kleindienst S, Gilbert JA, Handley K, Weisenhorn P, Overholt WA, Kostka JE. 2016. Responses of microbial communities to hydrocarbon exposures. Oceanography 29:136–149. https://doi.org/10.5670/oceanog.2016.78.
18. Prince RC, Amande TJ, McGenity TJ. 2018. Prokaryotic hydrocarbon degraders. *In* McGenity TJ (ed), Handbook of hydrocarbon and lipid microbiology. Springer, New York, NY. https://doi.org/10.1007/978-3-540-77587-4_118.
19. Yakimov MM, Timmis KN, Golyshin PN. 2007. Obligate oil-degrading marine bacteria. Curr Opin Biotechnol 18:257–266. https://doi.org/10.1016/j.copbio.2007.04.006.
20. Gutierrez T. 2019. Occurrence and roles of the obligate hydrocarbonoclastic bacteria in the ocean when there is no obvious hydrocarbon contamination, p 337–352. *In* McGenity T (ed), Taxonomy, genomics, and ecophysiology of hydrocarbon-degrading microbes: handbook of hydrocarbon and lipid microbiology. Springer, Cham, Switzerland. https://doi.org/10.1007/978-3-030-14796-9_14.
21. Head IM, Jones DM, Röling WF. 2006. Marine microorganisms make a meal of oil. Nat Rev Microbiol 4:173–182. https://doi.org/10.1038/nrmicro1348.
22. Hazen TC, Dubinsky EA, DeSantis TZ, Andersen GL, Piceno YM, Singh N, Jansson JK, Probst A, Borglin SE, Fortney JL, Stringfellow WT, Bill M, Conrad ME, Tom LM, Chavarria KL, Alusi TR, Lamendella R, Joyner DC, Spier C, Baelum J, Auer M, Zemla ML, Chakraborty R, Sonnenthal EL, D'haeseleer P, Holman H-YN, Osman S, Lu Z, Van Nostrand JD, Deng Y, Zhou J, Mason OU. 2010. Deep-sea oil plume enriches indigenous oil-degrading bacteria. Science 330:204–208. https://doi.org/10.1126/science.1195979.
23. Kleindienst S, Grim S, Sogin M, Bracco A, Crespo-Medina M, Joye SB. 2016. Diverse, rare microbial taxa responded to the Deepwater Horizon deep-sea hydrocarbon plume. ISME J 10:400–415. https://doi.org/10.1038/ismej.2015.121.
24. Ghosal D, Ghosh S, Dutta TK, Ahn Y. 2016. Current state of knowledge in microbial degradation of polycyclic aromatic hydrocarbons (PAHs): a review. Front Microbiol 7:1369.
25. Brakstad OG, Bonaunet K. 2006. Biodegradation of petroleum hydrocarbons in seawater at low temperatures (0–5°C) and bacterial communities associated with degradation. Biodegradation 17:71–82. https://doi.org/10.1007/s10532-005-3342-8.
26. Redmond MC, Valentine DL. 2012. Natural gas and temperature structured a microbial community response to the Deepwater Horizon oil spill. Proc Natl Acad Sci U S A 109:20292–20297. https://doi.org/10.1073/pnas.1108756108.
27. Ribicic D, McFarlin KM, Netzer R, Brakstad OG, Winkler A, Throne-Holst M, Størseth TR. 2018. Oil type and temperature-dependent biodegradation dynamics-combining chemical and microbial community data through multivariate analysis. BMC Microbiol 18:1–15. https://doi.org/10.1186/s12866-018-1221-9.
28. Prince RC, Butler JD, Redman AD. 2017. The rate of crude oil biodegradation in the sea. Environ Sci Technol 51:1278–1284. https://doi.org/10.1021/acs.est.6b03207.
29. Rojo F. 2009. Degradation of alkanes by bacteria. Environ Microbiol 11:2477–2490. https://doi.org/10.1111/j.1462-2920.2009.01948.x.
30. Ladino-Orjuela G, Gomes E, da Silva R, Salt C, Parsons JR. 2016. Metabolic pathways for degradation of aromatic hydrocarbons by bacteria. Rev

Environ Contam Toxicol 237:105–121. https://doi.org/10.1007/978-3-319-23573-8_5.
31. Atlas RM, Bartha R. 1972. Degradation and mineralization of petroleum in sea water: limitation by nitrogen and phosphorous. Biotechnol Bioeng 14:309–318. https://doi.org/10.1002/bit.260140304.
32. Swannell RP, Lee K, McDonagh M. 1996. Field evaluations of marine oil spill bioremediation. Microbiol Rev 60:342–365. https://doi.org/10.1128/mr.60.2.342-365.1996.
33. Rosenberg E, Ron EZ. 2005. Bioremediation of petroleum contamination, p 100–124. *In* Crawford RL, Crawford DL (ed), Bioremediation: principles and applications, vol 2. Cambridge University Press, Cambridge, United Kingdom.
34. Redfield AC. 1958. The biological control of chemical factors in the environment. Am Sci 46:205–221.
35. Ladousse A, Tramier B. 1991. Results of 12 years of research in spilled oil bioremediation: Inipol EAP 22. American Petroleum Institute: International Oil Spill Conference 1991:577–581. https://doi.org/10.7901/2169-3358-1991-1-577.
36. Jernelöv A, Lindén O. 1981. Ixtoc I: a case study of the world's largest oil spill. Ambio 10:299–306.
37. Mason OU, Scott NM, Gonzalez A, Robbins-Pianka A, Bælum J, Kimbrel J, Bouskill NJ, Prestat E, Borglin S, Joyner DC, Fortney JL, Jurelevicius D, Stringfellow WT, Alvarez-Cohen L, Hazen TC, Knight R, Gilbert JA, Jansson JK. 2014. Metagenomics reveals sediment microbial community response to Deepwater Horizon oil spill. ISME J 8:1464–1475. https://doi.org/10.1038/ismej.2013.254.
38. Harris KA, Yunker MB, Dangerfield N, Ross PS. 2011. Sediment-associated aliphatic and aromatic hydrocarbons in coastal British Columbia, Canada: concentrations, composition, and associated risks to protected sea otters. Environ Pollut 159:2665–2674. https://doi.org/10.1016/j.envpol.2011.05.033.
39. Beyer J, Trannum HC, Bakke T, Hodson PV, Collier TK. 2016. Environmental effects of the Deepwater Horizon oil spill: a review. Mar Pollut Bull 110:28–51. https://doi.org/10.1016/j.marpolbul.2016.06.027.
40. Nie Y, Chi CQ, Fang H, Liang JL, Lu SL, Lai GL, Tang YQ, Wu XL. 2014. Diverse alkane hydroxylase genes in microorganisms and environments. Sci Rep 4:4968–4911. https://doi.org/10.1038/srep04968.
41. Shao Z, Wang W. 2013. Enzymes and genes involved in aerobic alkane degradation. Front Microbiol 4:116. https://doi.org/10.3389/fmicb.2013.00116.
42. Seo JS, Keum YS, Li QX. 2009. Bacterial degradation of aromatic compounds. Int J Environ Res Public Health 6:278–309. https://doi.org/10.3390/ijerph6010278.
43. Ross MO, Rosenzweig AC. 2017. A tale of two methane monooxygenases. J Biol Inorg Chem 22:307–319. https://doi.org/10.1007/s00775-016-1419-y.
44. Dombrowski N, Donaho JA, Gutierrez T, Seitz KW, Teske AP, Baker BJ. 2016. Reconstructing metabolic pathways of hydrocarbon-degrading bacteria from the Deepwater Horizon oil spill. Nat Microbiol 1:16057–16057. https://doi.org/10.1038/nmicrobiol.2016.57.
45. Mounier J, Hakil F, Branchu P, Naïtali M, Goulas P, Sivadon P, Grimaud R. 2018. AupA and AupB are outer and inner membrane proteins involved in alkane uptake in *Marinobacter hydrocarbonoclasticus* SP17. mBio 9:e00520-18. https://doi.org/10.1128/mBio.00520-18.
46. Gibson DT, Koch JR, Kallio RE. 1968. Oxidative degradation of aromatic hydrocarbons by microorganisms. I. Enzymic formation of catechol from benzene. Biochemistry 7:2653–2662. https://doi.org/10.1021/bi00847a031.
47. Gutierrez T, Whitman WB, Huntemann M, Copeland A, Chen A, Kyrpides N, Markowitz V, Pillay M, Ivanova N, Mikhailova N, Ovchinnikova G, Andersen E, Pati A, Stamatis D, Reddy TBK, Ngan CY, Chovatia M, Daum C, Shapiro N, Cantor MN, Woyke T. 2015. Genome sequence of *Porticoccus hydrocarbonoclasticus* strain MCTG13d, an obligate polycyclic aromatic hydrocarbon-degrading bacterium associated with marine eukaryotic phytoplankton. Genome Announc 3:e00672-15. https://doi.org/10.1128/genomeA.00672-15.
48. Gutierrez T, Nichols PD, Whitman WB, Aitken MD. 2012. *Porticoccus hydrocarbonoclasticus* sp. nov., an aromatic hydrocarbon-degrading bacterium identified in laboratory cultures of marine phytoplankton. Appl Environ Microbiol 78:628–637. https://doi.org/10.1128/AEM.06398-11.
49. Lea-Smith DJ, Biller SJ, Davey MP, Cotton CA, Sepulveda BMP, Turchyn AV, Scanlan DJ, Smith AG, Chisholm SW, Howe CJ. 2015. Contribution of cyanobacterial alkane production to the ocean hydrocarbon cycle. Proc Natl Acad Sci U S A 112:13591–13596. https://doi.org/10.1073/pnas.1507274112.
50. Koo H, Mojib N, Huang JP, Donahoe RJ, Bej AK. 2015. Bacterial community shift in the coastal Gulf of Mexico salt-marsh sediment microcosm *in vitro* following exposure to the Mississippi Canyon Block 252 oil (MC252). 3 Biotech 5:379–392. https://doi.org/10.1007/s13205-014-0233-x.
51. Miller JI, Techtmann S, Fortney J, Mahmoudi N, Joyner D, Liu J, Olesen S, Alm E, Fernandez A, Gardinali P, GaraJayeva N, Askerov FS, Hazen TC. 2019. Oil hydrocarbon degradation by Caspian Sea microbial communities. Front Microbiol 10:995. https://doi.org/10.3389/fmicb.2019.00995.
52. Bagi A, Pampanin DM, Lanzén A, Bilstad T, Kommedal R. 2014. Naphthalene biodegradation in temperate and arctic marine microcosms. Biodegradation 25:111–125. https://doi.org/10.1007/s10532-013-9644-3.
53. Yuan C, Lei J, Cole J, Sun Y. 2015. Reconstructing 16S rRNA genes in metagenomic data. Bioinformatics 31:i35–i43. https://doi.org/10.1093/bioinformatics/btv231.
54. Baas-Becking LGM. 1934. Geobiologie of inleiding tot de milieukunde. WP Van Stockum & Zoon NV, Amsterdam, Netherlands.
55. Yoon J-H, Park S, Jung Y-T, Lee J-S, Lee K-C. 2013. *Paraperlucidibaca wandonensis* sp. nov., isolated from seawater, and emended description of the genus *Paraperlucidibaca* Oh et al. 2011. Int J Syst Evol Microbiol 63:4113–4117. https://doi.org/10.1099/ijs.0.048645-0.
56. Oh KH, Lee SY, Lee MH, Oh TK, Yoon JH. 2011. *Paraperlucidibaca baekdonensis* gen. nov., sp. nov., isolated from seawater. Int J Syst Evol Microbiol 61:1382–1385. https://doi.org/10.1099/ijs.0.023994-0.
57. Kasai Y, Kishira H, Harayama S. 2002. Bacteria belonging to the genus *Cycloclasticus* play a primary role in the degradation of aromatic hydrocarbons released in a marine environment. Appl Environ Microbiol 68:5625–5633. https://doi.org/10.1128/AEM.68.11.5625-5633.2002.
58. Chung WK, King GM. 2001. Isolation, characterization, and polyaromatic hydrocarbon degradation potential of aerobic bacteria from marine macrofaunal burrow sediments and description of *Lutibacterium anuloederans* gen. nov., sp. nov., and *Cycloclasticus spirillensus* sp. nov. Appl Environ Microbiol 67:5585–5592. https://doi.org/10.1128/AEM.67.12.5585-5592.2001.
59. Rubin-Blum M, Antony CP, Borowski C, Sayavedra L, Pape T, Sahling H, Bohrmann G, Kleiner M, Redmond MC, Valentine DL, Dubilier N. 2017. Short-chain alkanes fuel mussel and sponge *Cycloclasticus* symbionts from deep-sea gas and oil seeps. Nat Microbiol 2:17093–17011. https://doi.org/10.1038/nmicrobiol.2017.93.
60. Gutierrez T, Morris G, Ellis D, Bowler B, Jones M, Salek K, Mulloy B, Teske A. 2018. Hydrocarbon-degradation and MOS-formation capabilities of the dominant bacteria enriched in sea surface oil slicks during the Deepwater Horizon oil spill. Mar Pollut Bull 135:205–215. https://doi.org/10.1016/j.marpolbul.2018.07.027.
61. Schreiber L, Fortin N, Tremblay J, Wasserscheid J, Sanschagrin S, Mason J, Wright CA, Spear D, Johannessen SC, Robinson B, King T, Lee K, Greer CW. 2021. In situ microcosms deployed at the coast of British Columbia (Canada) to study dilbit weathering and associated microbial communities under marine conditions. FEMS Microbiol Ecol 97:fiab082. https://doi.org/10.1093/femsec/fiab082.
62. Schubotz F, Lipp JS, Elvert M, Kasten S, Mollar XP, Zabel M, Bohrmann G, Hinrichs KU. 2011. Petroleum degradation and associated microbial signatures at the Chapopote asphalt volcano, Southern Gulf of Mexico. Geochim Cosmochim Acta 75:4377–4398. https://doi.org/10.1016/j.gca.2011.05.025.
63. Redmond MC, Valentine DL, Sessions AL. 2010. Identification of novel methane-, ethane-, and propane-oxidizing bacteria at marine hydrocarbon seeps by stable isotope probing. Appl Environ Microbiol 76:6412–6422. https://doi.org/10.1128/AEM.00271-10.
64. Rivers AR, Sharma S, Tringe SG, Martin J, Joye SB, Moran MA. 2013. Transcriptional response of bathypelagic marine bacterioplankton to the Deepwater Horizon oil spill. ISME J 7:2315–2329. https://doi.org/10.1038/ismej.2013.129.
65. Valentine DL, Kessler JD, Redmond MC, Mendes SD, Heintz MB, Farwell C, Hu L, Kinnaman FS, Yvon-Lewis S, Du M, Chan EW, Tigreros FG, Villanueva CJ. 2010. Propane respiration jump-starts microbial response to a deep oil spill. Science 330:208–211. https://doi.org/10.1126/science.1196830.
66. Joye SB, MacDonald IR, Leifer I, Asper V. 2011. Magnitude and oxidation potential of hydrocarbon gases released from the BP oil well blowout. Nature Geosci 4:160–164. https://doi.org/10.1038/ngeo1067.
67. Gutierrez T, Singleton DR, Berry D, Yang T, Aitken MD, Teske A. 2013. Hydrocarbon-degrading bacteria enriched by the Deepwater Horizon oil spill identified by cultivation and DNA-SIP. ISME J 7:2091–2104. https://doi.org/10.1038/ismej.2013.98.

68. Yakimov MM, Giuliano L, Gentile G, Crisafi E, Chernikova TN, Abraham WR, Lünsdorf H, Timmis KN, Golyshin PN. 2003. *Oleispira antarctica* gen. nov., sp. nov., a novel hydrocarbonoclastic marine bacterium isolated from Antarctic coastal sea water. Int J Syst Evol Microbiol 53:779–785. https://doi.org/10.1099/ijs.0.02366-0.
69. Wang Y, Yu M, Austin B, Zhang XH. 2012. *Oleispira lenta* sp. nov., a novel marine bacterium isolated from Yellow sea coastal seawater in Qingdao, China. Antonie Van Leeuwenhoek 101:787–794. https://doi.org/10.1007/s10482-011-9693-8.
70. Yakimov MM, Giuliano L, Denaro R, Crisafi E, Chernikova TN, Abraham WR, Lünsdorf H, Timmis KN, Golyshin PN, Golyshin PN. 2004. *Thalassolituus oleivorans* gen. nov., sp. nov., a novel marine bacterium that obligately utilizes hydrocarbons. Int J Syst Evol Microbiol 54:141–148. https://doi.org/10.1099/ijs.0.02424-0.
71. Golyshin PN, Werner J, Chernikova TN, Tran H, Ferrer M, Yakimov MM, Teeling H, Golyshina OV, MAMBA Scientific Consortium. 2013. Genome sequence of *Thalassolituus oleivorans* MIL-1 (DSM 14913T). Genome Announc 1:e00141-13. https://doi.org/10.1128/genomeA.00141-13.
72. Kube M, Chernikova TN, Al-Ramahi Y, Beloqui A, Lopez-Cortez N, Guazzaroni ME, Heipieper HJ, Klages S, Kotsyurbenko OR, Langer I, Nechitaylo TY, Lünsdorf H, Fernández M, Juárez S, Ciordia S, Singer A, Kagan O, Egorova O, Petit PA, Stogios P, Kim Y, Tchigvintsev A, Flick R, Denaro R, Genovese M, Albar JP, Reva ON, Martínez-Gomariz M, Tran H, Ferrer M, Savchenko A, Yakunin AF, Yakimov MM, Golyshina OV, Reinhardt R, Golyshin PN. 2013. Genome sequence and functional genomic analysis of the oil-degrading bacterium *Oleispira antarctica*. Nat Commun 4:2156. https://doi.org/10.1038/ncomms3156.
73. Joye SB, Teske AP, Kostka JE. 2014. Microbial dynamics following the Macondo oil well blowout across Gulf of Mexico environments. Bioscience 64:766–777. https://doi.org/10.1093/biosci/biu121.
74. Parks DH, Chuvochina M, Waite DW, Rinke C, Skarshewski A, Chaumeil PA, Hugenholtz P. 2018. A standardized bacterial taxonomy based on genome phylogeny substantially revises the tree of life. Nat Biotechnol 36:996–1004. https://doi.org/10.1038/nbt.4229.
75. Parks DH, Chuvochina M, Chaumeil PA, Rinke C, Mussig AJ, Hugenholtz P. 2020. A complete domain-to-species taxonomy for *Bacteria* and *Archaea*. Nat Biotechnol 38:1079–1086. https://doi.org/10.1038/s41587-020-0501-8.
76. Lo N, Kang HJ, Jeon CO. 2014. *Zhongshania aliphaticivorans* sp. nov., an aliphatic hydrocarbon-degrading bacterium isolated from marine sediment, and transfer of *Spongiibacter borealis* Jang et al. 2011 to the genus *Zhongshania* as *Zhongshania borealis* comb. nov. Int J Syst Evol Microbiol 64:3768–3774. https://doi.org/10.1099/ijs.0.068593-0.
77. Ribicic D, Netzer R, Hazen TC, Techtmann SM, Drabløs F, Brakstad OG. 2018. Microbial community and metagenome dynamics during biodegradation of dispersed oil reveals potential key-players in cold Norwegian seawater. Mar Pollut Bull 129:370–378. https://doi.org/10.1016/j.marpolbul.2018.02.034.
78. Barbato M, Scoma A. 2020. Mild hydrostatic-pressure (15 MPa) affects the assembly, but not the growth, of oil-degrading coastal microbial communities tested under limiting conditions (5°C, no added nutrients). FEMS Microbiol Ecol 96:fiaa160. https://doi.org/10.1093/femsec/fiaa160.
79. Jang GI, Hwang CY, Choi HG, Kang SH, Cho BC. 2011. Description of *Spongiibacter borealis* sp. nov., isolated from Arctic seawater, and reclassification of Melitea salexigens Urios et al. 2008 as a later heterotypic synonym of *Spongiibacter marinus* Graeber et al. 2008 with emended descriptions of the genus *Spongiibacter* and *Spongiibacter marinus*. Int J Syst Evol Microbiol 61:2895–2900. https://doi.org/10.1099/ijs.0.028795-0.
80. Li HJ, Zhang XY, Chen CX, Zhang YJ, Gao ZM, Yu Y, Chen XL, Chen B, Zhang YZ. 2011. *Zhongshania antarctica* gen. nov., sp. nov. and *Zhongshania guokunii* sp. nov., gammaproteobacteria respectively isolated from coastal attached (fast) ice and surface seawater of the Antarctic. Int J Syst Evol Microbiol 61:2052–2057. https://doi.org/10.1099/ijs.0.026153-0.
81. Ławniczak Ł, Woźniak-Karczewska M, Loibner AP, Heipieper HJ, Chrzanowski Ł. 2020. Microbial degradation of hydrocarbons—basic principles for bioremediation: a review. Molecules 25:856. https://doi.org/10.3390/molecules25040856.
82. Zhu X, Venosa AD, Suidan MT, Lee K. 2001. Guidelines for the bioremediation of marine shorelines and freshwater wetlands. US Environmental Protection Agency, Washington, DC. https://www.epa.gov/sites/production/files/2013-07/documents/guidelines_for_the_bioremediation_of_marine_shorelines_and_freshwater_wetlands.pdf.
83. Atlas RM, Bragg J. 2009. Bioremediation of marine oil spills: when and when not—the Exxon Valdez experience. Microb Biotechnol 2:213–221. https://doi.org/10.1111/j.1751-7915.2008.00079.x.
84. Bragg JR, Prince RC, Harner EJ, Atlas RM. 1994. Effectiveness of bioremediation for the Exxon Valdez oil spill. Nature 368:413–418. https://doi.org/10.1038/368413a0.
85. Kasai Y, Kishira H, Sasaki T, Syutsubo K, Watanabe K, Harayama S. 2002. Predominant growth of *Alcanivorax* strains in oil-contaminated and nutrient-supplemented sea water. Environ Microbiol 4:141–147. https://doi.org/10.1046/j.1462-2920.2002.00275.x.
86. Sun Y, Wang H, Li J, Wang B, Qi C, Hu X. 2018. Nutrient-enhanced *n*-alkanes biodegradation and succession of bacterial communities. J Ocean Limnol 36:1294–1303. https://doi.org/10.1007/s00343-018-6310-y.
87. Heipieper HJ, Martínez PM. 2010. Toxicity of hydrocarbons to microorganisms, p 1563–1573. *In* Timmis KN (ed), Handbook of hydrocarbon and lipid microbiology. Springer, Berlin, Germany. https://doi.org/10.1007/978-3-540-77587-4_108.
88. Rambeloarisoa E, Rontani JF, Giusti G, Duvnjak Z, Bertrand JC. 1984. Degradation of crude oil by a mixed population of bacteria isolated from sea-surface foams. Mar Biol 83:69–81. https://doi.org/10.1007/BF00393087.
89. Zahed MA, Aziz HA, Isa MH, Mohajeri L. 2010. Effect of initial oil concentration and dispersant on crude oil biodegradation in contaminated seawater. Bull Environ Contam Toxicol 84:438–442. https://doi.org/10.1007/s00128-010-9954-7.
90. Atlas RM. 2007. Microbial hydrocarbon degradation-bioremediation of oil spills. J Chem Technol Biotechnol 52:149–156. https://doi.org/10.1002/jctb.280520202.
91. Pritchard PH, Mueller JG, Rogers JC, Kremer FV, Glaser JA. 1992. Oil spill bioremediation: experiences, lessons and results from the Exxon Valdez oil spill in Alaska. Biodegradation 3:315–335. https://doi.org/10.1007/BF00129091.
92. Prince RC, McFarlin KM, Butler JD, Febbo EJ, Wang FC, Nedwed TJ. 2013. The primary biodegradation of dispersed crude oil in the sea. Chemosphere 90:521–526. https://doi.org/10.1016/j.chemosphere.2012.08.020.
93. Brakstad OG, Nonstad I, Faksness LG, Brandvik PJ. 2008. Responses of microbial communities in Arctic sea ice after contamination by crude petroleum oil. Microb Ecol 55:540–552. https://doi.org/10.1007/s00248-007-9299-x.
94. Passow U, Ziervogel K, Asper V, Diercks A. 2012. Marine snow formation in the aftermath of the Deepwater Horizon oil spill in the Gulf of Mexico. Environ Res Lett 7:e035301. https://doi.org/10.1088/1748-9326/7/3/035301.
95. Passow U, Ziervogel K. 2016. Marine snow sedimented oil released during the Deepwater Horizon spill. Oceanog 29:118–125. https://doi.org/10.5670/oceanog.2016.76.
96. Babcock-Adams L, Chanton JP, Joye SB, Medeiros PM. 2017. Hydrocarbon composition and concentrations in the Gulf of Mexico sediments in the 3 years following the Macondo well blowout. Environ Pollut 229:329–338. https://doi.org/10.1016/j.envpol.2017.05.078.
97. Romero IC, Toro-Farmer G, Diercks AR, Schwing P, Muller-Karger F, Murawski S, Hollander DJ. 2017. Large-scale deposition of weathered oil in the Gulf of Mexico following a deep-water oil spill. Environ Pollut 228:179–189. https://doi.org/10.1016/j.envpol.2017.05.019.
98. Oldenburg TBP, Jaeger P, Gros J, Socolofsky SA, Pesch S, Radović J, Jaggi A. 2020. Physical and chemical properties of oil and gas under reservoir and deep-sea conditions, p 25–42. *In* Murawski SA, Ainsworth C, Gilbert S, Hollander D, Paris CB, Schlüter M, Wetzel D (ed), Deep oil spills: facts, fate and effects. Springer Nature Switzerland AG, Cham, Switzerland. https://doi.org/10.1007/978-3-030-11605-7.
99. Widdel F, Bak F. 1992. Gram-negative mesophilic sulfate-reducing bacteria, p 3352–3378. *In* Balows H, Triiper HG, Dworkin M, Harder W, Schleifer KH (ed), The prokaryotes, 2nd ed, vol 4. Springer Verlag, New York, NY.
100. Wheeler PA, Watkins JM, Hansing RL. 1997. Nutrients, organic carbon and organic nitrogen in the upper water column of the Arctic Ocean: implications for the sources of dissolved organic carbon. Deep Sea Res 2 Top Stud Oceanogr 44:1571–1592. https://doi.org/10.1016/S0967-0645(97)00051-9.
101. McIntyre CP, Harvey PM, Ferguson SH, Wressnig AM, Volk H, George SC, Snape I. 2007. Determining the extent of biodegradation of fuels using the diastereomers of acyclic isoprenoids. Environ Sci Technol 41:2452–2458. https://doi.org/10.1021/es0621288.
102. Bayona JM, Albaiges J, Solanas AM, Pares R, Garrigues P, Ewald M. 1986. Selective aerobic degradation of methyl-substituted polycyclic aromatic hydrocarbons in petroleum by pure microbial cultures. Int J Environ Anal Chem 23:289–303. https://doi.org/10.1080/03067318608076451.

103. Townsend GT, Prince RC, Suflita JM. 2004. Anaerobic biodegradation of alicyclic constituents of gasoline and natural gas condensate by bacteria from an anoxic aquifer. FEMS Microbiol Ecol 49:129–135. https://doi.org/10.1016/j.femsec.2003.08.015.
104. Prince RC, Elmendorf DL, Lute JR, Hsu CS, Haith CE, Senius JD, Dechert GJ, Douglas GS, Butler EL. 1994. 17α(H)-21β(H)-hopane as a conserved internal marker for estimating the biodegradation of crude oil. Environ Sci Technol 28:142–145. https://doi.org/10.1021/es00050a019.
105. Prince RC, Bare RE, Garrett RM, Grossman MJ, Haith CE, Keim LG, Lee K, Holtom GJ, Lambert P, Sergy GA, Owens EH, Guénette CC. 2003. Bioremediation of stranded oil on an Arctic shoreline. Spill Sci Technol Bull 8:303–312. https://doi.org/10.1016/S1353-2561(03)00036-7.
106. Klindworth A, Pruesse E, Schweer T, Peplies J, Quast C, Horn M, Glöckner FO. 2013. Evaluation of general 16S ribosomal RNA gene PCR primers for classical and next-generation sequencing-based diversity studies. Nucleic Acids Res 41:e1. https://doi.org/10.1093/nar/gks808.
107. Caporaso JG, Lauber CL, Walters WA, Berg-Lyons D, Lozupone CA, Turnbaugh PJ, Fierer N, Knight R. 2011. Global patterns of 16S rRNA diversity at a depth of millions of sequences per sample. Proc Natl Acad Sci U S A 108(Suppl 1):4516–4522. https://doi.org/10.1073/pnas.1000080107.
108. Acinas SG, Sarma-Rupavtarm R, Klepac-Ceraj V, Polz MF. 2005. PCR-induced sequence artifacts and bias: insights from comparison of two 16S rRNA clone libraries constructed from the same sample. Appl Environ Microbiol 71:8966–8969. https://doi.org/10.1128/AEM.71.12.8966-8969.2005.
109. Sharp CE, Urschel S, Dong X, Brady AL, Slater GF, Strous M. 2017. Robust, high-productivity phototrophic carbon capture at high pH and alkalinity using natural microbial communities. Biotechnol Biofuels 10:84. https://doi.org/10.1186/s13068-017-0769-1.
110. Dong X, Kleiner M, Sharp CE, Thorson E, Li C, Liu D, Strous M. 2017. Fast and simple analysis of MiSeq amplicon sequencing data with MetaAmp. Front Microbiol 8:1461. https://doi.org/10.3389/fmicb.2017.01461.
111. Li D, Luo R, Liu CM, Leung CM, Ting HF, Sadakane K, Yamashita H, Lam TW. 2016. MEGAHIT v1.0: a fast and scalable metagenome assembler driven by advanced methodologies and community practices. Methods 102:3–11. https://doi.org/10.1016/j.ymeth.2016.02.020.
112. Kang DD, Li F, Kirton E, Thomas A, Egan R, An H, Wang Z. 2019. MetaBAT 2: an adaptive binning algorithm for robust and efficient genome reconstruction from metagenome assemblies. PeerJ 7:e7359. https://doi.org/10.7717/peerj.7359.
113. Parks DH, Imelfort M, Skennerton CT, Hugenholtz P, Tyson GW. 2015. CheckM: assessing the quality of microbial genomes recovered from isolates, single cells, and metagenomes. Genome Res 25:1043–1055. https://doi.org/10.1101/gr.186072.114.
114. Chaumeil PA, Mussig AJ, Hugenholtz P, Parks DH. 2020. GTDB-Tk: a toolkit to classify genomes with the Genome Taxonomy Database. Bioinformatics 36:1925–1927.
115. Price MN, Dehal PS, Arkin AP. 2010. FastTree 2: approximate maximum-likelihood trees for large alignments. PLoS One 5:e9490. https://doi.org/10.1371/journal.pone.0009490.
116. Dong X, Strous M. 2019. An integrated pipeline for annotation and visualization of metagenomic contigs. Front Genet 10:999. https://doi.org/10.3389/fgene.2019.00999.
117. Altschul SF, Gish W, Miller W, Myers EW, Lipman DJ. 1990. Basic local alignment search tool. J Mol Biol 215:403–410. https://doi.org/10.1016/S0022-2836(05)80360-2.
118. Jain C, Rodriguez-R LM, Phillippy AM, Konstantinidis KT, Aluru S. 2018. High throughput ANI analysis of 90K prokaryotic genomes reveals clear species boundaries. Nat Commun 9:1–8. https://doi.org/10.1038/s41467-018-07641-9.
119. Nayfach S, Shi ZJ, Seshadri R, Pollard KS, Kyrpides NC. 2019. New insights from uncultivated genomes of the global human gut microbiome. Nature 568:505–510. https://doi.org/10.1038/s41586-019-1058-x.
120. R Core Team. 2019. R: a language and environment for statistical computing. R Foundation for Statistical Computing, Vienna, Austria. https://www.R-project.org/.
121. Oksanen J, Blanchet G, Friendly M, Kindt R, Legendre P, McGlinn D, Minchin P, O'Hara R, Simpson G, Solymos P, Henry M, Stevens H, Szoecs E, Wagner H. 2018 Vegan: Community Ecology Package. R package version 2.5-3.
122. Clarke KR. 1993. Non-parametric multivariate analyses of changes in community structure. Austral Ecol 18:117–143. https://doi.org/10.1111/j.1442-9993.1993.tb00438.x.
123. De Cáceres M, Legendre P. 2009. Associations between species and groups of sites: indices and statistical inference. Ecology 90:3566–3574. https://doi.org/10.1890/08-1823.1.